Waveform focal mechanisms for Hungary

Zoltán Wéber

Kövesligethy Radó Seismological Observatory
CSFK GGI
Eötvös Loránd Research Network
weber@seismology.hu

Budapest
December 20, 2020

This work was financially supported by the National Research, Development and Innovation Fund, Hungary (K124241 and 2018-1.2.1-NKP-2018-00007).

Contents

1 Introduction

This booklet presents a preliminary catalog of earthquake focal mechanisms for Hungary (central part of the Pannonian basin). We used probabilistic non-linear waveform inversion methods Wéber (2005, 2006, 2009, 2018) to retrieve both the centroids and the moment tensors of the investigated local and near-regional earthquakes. The uncertainties of the resulting source parameters are estimated as well. The moment tensor solutions described in this booklet are robust and of sufficient quality to draw conclusions on the neotectonic features of the epicentral regions.

If you use the focal mechanism data published here, please cite one or more of the following papers:

- Wéber Z, 2006. Probabilistic local waveform inversion for moment tensor and hypocentral location. *Geophys. J. Int.* 165, 607-621. doi: 10.1111/j.1365-246X.2006.02934.x
- Wéber Z, 2009. Estimating source time function and moment tensor from moment tensor rate functions by constrained L1 norm minimization. *Geophys. J. Int.* 178, 889-900. doi: 10.1111/j.1365-246X.2009.04202.x
- Wéber Z, Süle B, 2014. Source properties of the 29 January 2011 ML 4.5 Oroszlány (Hungary) mainshock and its aftershocks. *Bull. Seismol. Soc. Am.* 104, 113-127. doi: 10.1785/0120130152
- Wéber Z, 2016a. Probabilistic waveform inversion for 22 earthquake moment tensors in Hungary: new constraints on the tectonic stress pattern inside the Pannonian basin. *Geophys. J. Int.* 204, 236-249. doi: 10.1093/gji/ggv446
- Wéber Z, 2016b. Source parameters for the 2013–2015 earthquake sequence in Nógrád county, Hungary. *J. Seismol.* 20, 987-999. doi: 10.1007/s10950-016-9576-6
- Wéber Z, 2018. Probabilistic joint inversion of waveforms and polarity data for double-couple focal mechanisms of local earthquakes. *Geophys. J. Int.* 213, 1586-1598. doi: 10.1093/gji/ggy096
- Wéber Z, Czecze B, Süle B, Bondár I, AlpArray Working Group, 2020. Source analysis of the March 7, 2019 $M_L = 4.0$ Somogyszob, Hungary earthquake sequence. *Acta Geod. Geophys.* 55, 371-387. doi: 10.1007/s40328-020-00311-7

This preliminary catalog is regularly updated and made available on-line at
http://nkp.ggki.hu/results.

2 Inversion methods

To determine the focal mechanisms for the selected earthquakes, we applied the Monte Carlo Moment Tensor (MCMT) inversion method (Wéber, 2006, 2009) and the Joint Waveform and Polarity (JOWAPO) inversion technique (Wéber, 2018). They have already been successfully applied for studying the source mechanisms of both local and near-regional events in the Pannonian basin (Wéber and Süle, 2014; Wéber, 2016a,b, 2020). The procedures work in the point-source approximation and are summarized briefly in the following paragraphs.

2.1 Monte Carlo Moment Tensor (MCMT) inversion

We describe a general seismic point source by a moment tensor (MT) and a source time function (STF). In general, the MT has six independent components. If the velocity structure and the hypocentral coordinates are known, there is a linear connection between the seismograms and the MT. More specifically, if the STF is known or assumed to be known, the MT is calculated by deconvolving the station specific Green's functions (GFs) from the observed seismograms. For the generation of the synthetic GFs, we use the software tools from the "Computer Programs in Seismology" open source package (Herrmann, 2013). We applied the propagator matrix–wavenumber integration method, which allows calculating the entire wavefield for horizontally layered earth structures at high frequencies and short epicentral distances. For events in the Pannonian basin we calculate the synthetic waveforms from a recently developed one-dimensional (1D) velocity model (Gráczer and Wéber, 2012).

In the first step of the MCMT inversion, we apply a simple grid-search algorithm to map the posterior probability density (PPD) of the hypocenter using the travel time hypocenter as *a priori* information and the observed waveforms as data. Hypocenter errors, measurement errors and modeling errors lead to uncertain inversion results. Therefore, in the next step we estimate the overall uncertainties of the retrieved MT using a Monte Carlo simulation technique (Rubinstein and Kroese, 2008). Monte Carlo simulation determines how random variation in the input data affects the uncertainty of the output. In our problem, the simulation generates many new realizations of input data sets by randomly generating new hypocenters and waveforms according to their respective distributions. Then each generated input data set is inverted for MT (output). The distribution of the obtained set of MT solutions approximates well the PPD of the MT. In this study, we performed 10,000 Monte Carlo simulations and thus generated 10,000 MTs according to its posterior distribution. The final estimate for the best MT is given by the maximum likelihood point.

After obtaining an ensemble of MT solutions, we calculate the principal axes for each member mechanism of the ensemble. We adopt the convention of Sipkin (1993) that the P and T axes always point upwards and the principal axes form a right-handed coordinate system. Then we construct the two-dimensional histograms of the principal axes on the focal sphere and determine the confidence zones for the 50, 68, 90 and 95% confidence levels. The confidence contours of the P and T principal axes are then plotted on top of the beach ball representation of the maximum likelihood mechanism.

Additionally, each MT in the ensemble is decomposed into a double-couple (DC), a compensated linear vector dipole (CLVD), and an isotropic (ISO) component (Jost and Herrmann, 1989). To assess the relative amounts of these components in a MT, we calculate their percentages as well.

The scalar seismic moments of the ISO, CLVD and DC components of a general moment

tensor **M** are determined according to Vavryčuk (2015):

$$M_{ISO} = \frac{1}{3}(\lambda_1 + \lambda_2 + \lambda_3) \tag{1}$$

$$M_{CLVD} = \frac{2}{3}(\lambda_1 + \lambda_3 - 2\lambda_2) \tag{2}$$

$$M_{DC} = \frac{1}{2}(\lambda_1 - \lambda_3 - |\lambda_1 + \lambda_3 - 2\lambda_2|) \tag{3}$$

where $\lambda_1 \geq \lambda_2 \geq \lambda_3$ denote the eigenvalues of **M**. Positive ISO moment means explosion, whereas negative moment means implosion. The CLVD moment also includes the sign of the elementary CLVD tensor: positive moment means CLVD component with major dipole directed along the T-axis, whereas negative moment means CLVD component with major dipole directed along the P-axis. Note that the above equations are equivalent to those published by Jost and Herrmann (1989).

The scalar seismic moment of a general moment tensor is then defined as

$$M_0 = M_{DC} + |M_{CLVD}| + |M_{ISO}|. \tag{4}$$

The same value of M_0 is produced by the norm proposed by Bowers and Hudson (1999).

To assess the relative amounts of the DC, CLVD and ISO components, we calculate their percentages in the following way:

$$P_{DC} = \frac{M_{DC}}{M_0} \times 100 \ \ (\%) \tag{5}$$

$$P_{CLVD} = \frac{M_{CLVD}}{M_0} \times 100 \ \ (\%) \tag{6}$$

$$P_{ISO} = \frac{M_{ISO}}{M_0} \times 100 \ \ (\%) \tag{7}$$

The ISO and CLVD components are called the non-DC components of **M**. Due to noise in the observed seismograms, as well as the inaccurate knowledge of the Green's functions, waveform inversion always produces earthquake mechanisms with non-DC components.

We also compute the moment magnitude M_w from the scalar seismic moment M_0 according to the definition of Hanks and Kanamori (1979):

$$M_w = \frac{2}{3}\log M_0 - 6.03 \tag{8}$$

where M_0 is measured in Nm.

2.2 Joint Waveform and Polarity (JOWAPO) inversion

When inverting for the mechanism of low-magnitude local events, we have to use relatively high-frequency (>0.5 Hz) waveforms. At high frequencies, however, the GFs can be modeled satisfactorily only for relatively near stations, because the velocity model is usually not detailed enough to model complex GFs at large epicentral distances. Unfortunately, it is a common scenario that the number of the high-quality near-station seismograms is not enough for successful waveform inversion. Using polarity data and waveforms together can be a remedy to this problem. In this study we apply the Joint Waveform and Polarity (JOWAPO) inversion technique (Wéber,

2018) when the analyzed earthquake does not have the required number of high-quality near-station seismograms for pure waveform inversion.

The JOWAPO method is able to estimate the DC mechanism of the studied earthquake. It defines a likelihood function for both polarities and waveforms, and then performs Bayesian sampling. Bayesian sampling generates an ensemble of DC focal mechanisms whose members are distributed according to the PPD of the model parameters. We assume no prior information on the model parameters. As is shown in Wéber (2018), the prior probability density is constant if the model parameters are $(\phi, \cos\delta, \lambda)$, where ϕ denotes the strike, δ the dip and λ the rake of a DC mechanism. Thus, the JOWAPO method generates an ensemble of DC focal mechanisms in the 3D $(\phi, \cos\delta, \lambda)$ model space. Using waveforms in the inversion makes it possible to estimate the optimal source depth and the seismic scalar moment as well. The method can utilize any type of first-motion data (P, SV and SH polarities) and can invert polarities without waveforms or vice versa.

For full details of the MCMT and JOWAPO inversion methods, the reader is referred to Wéber (2006, 2016a,b, 2018).

3 Focal mechanism solutions

3.1 Map overview

Figure 1 summarizes the source mechanisms of the studied earthquakes on a map of Hungary.

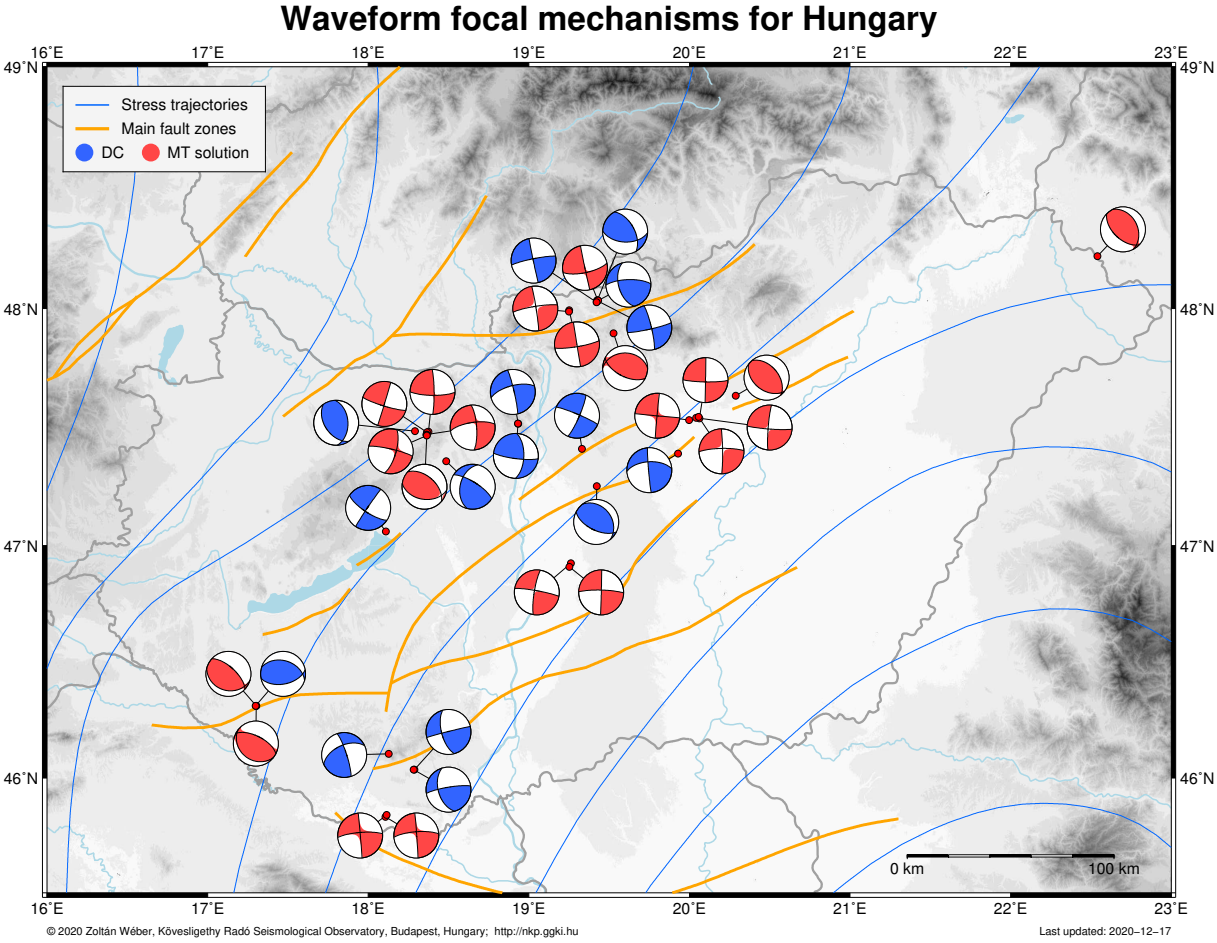

Figure 1: Source mechanisms of the analyzed earthquakes on a map of Hungary (red: MCMT solutions; blue: JOWAPO solutions; shaded area: compression; open area: dilatation). Equal area projection of lower hemisphere is used. Thin blue lines depict the trajectories of maximum horizontal stress directions after Bada et al. (2007), whereas thick orange lines indicate main active fault zones after Horváth et al. (2006).

3.2 List overview

The table below lists the centroids, moment magnitudes and source mechanisms for the investigated earthquakes. Red beach balls denote MT mechanisms derived by MCMT, whereas blue beach balls represent DC mechanisms estimated by JOWAPO. Click on a beach ball to access the detailed focal mechanism description for the selected event.

No.	Date	Time	Lon. (°E)	Lat. (°N)	Depth (km)	M_w	Mechanism
1	1985-08-15	04:28:47	18.110	47.060	12	5.01	
2	1995-06-09	15:57:02	19.262	46.924	13	2.18	
3	1996-03-28	06:31:22	19.252	46.909	11	2.94	
4	1997-05-23	23:40:18	18.486	47.358	12	2.18	
5	1997-11-27	10:40:56	19.424	47.252	13	2.99	
6	1998-05-08	04:06:54	18.933	47.516	9	2.44	
7	1998-06-28	12:19:39	18.933	47.517	8	1.87	
8	2001-05-25	15:15:49	18.107	45.832	13	1.89	
9	2001-06-08	09:58:56	18.114	45.840	12	1.84	
10	2002-02-22	11:52:34	18.291	47.485	6	2.77	
11	2002-10-12	18:49:11	20.062	47.539	14	2.91	
12	2002-10-23	02:52:15	20.041	47.541	14	3.41	
13	2003-06-21	20:05:58	20.058	47.545	14	3.32	
14	2003-06-27	01:19:20	19.998	47.531	10	2.39	
15	2003-08-31	22:57:21	18.127	46.105	4	2.74	
16	2003-12-31	20:43:49	18.288	46.037	13	2.61	

On-line: http://nkp.ggki.hu/results

No.	Date	Time	Lon. (°E)	Lat. (°N)	Depth (km)	M_w	Mechanism
17	2003-12-31	21:36:02	18.283	46.037	10	2.02	
18	2004-06-19	10:48:07	19.930	47.390	13	2.62	
19	2004-09-29	00:46:27	19.527	47.897	8	2.39	
20	2006-11-23	07:15:21	22.541	48.218	11	4.08	
21	2006-12-31	13:39:23	19.331	47.410	6	3.34	
22	2011-01-29	17:41:38	18.375	47.482	7	4.17	
23	2011-01-30	13:34:28	18.366	47.480	8	2.17	
24	2011-01-30	20:58:45	18.363	47.471	8	2.56	
25	2011-01-31	00:25:29	18.365	47.469	8	2.46	
26	2011-03-11	01:45:23	18.365	47.467	8	2.45	
27	2013-04-22	22:28:46	20.289	47.634	3	4.46	
28	2013-06-05	18:45:46	19.251	47.992	3	3.90	
29	2013-07-02	19:07:32	19.250	47.987	3	3.67	
30	2014-01-19	01:34:34	19.429	48.035	4	4.02	
31	2014-01-19	01:48:43	19.424	48.033	3	3.16	
32	2014-08-03	01:48:48	19.423	48.029	4	3.01	
33	2015-01-01	06:43:23	19.431	48.033	4	3.70	
34	2015-01-01	10:45:57	19.422	48.026	6	3.75	
35	2019-02-17	14:40:45	17.303	46.312	11	2.58	

On-line: http://nkp.ggki.hu/results

No.	Date	Time	Lon. (°E)	Lat. (°N)	Depth (km)	M_w	Mechanism
36	2019-03-07	19:07:53	17.302	46.312	11	3.79	
37	2019-04-05	13:52:32	17.299	46.312	11	2.69	

3.3 Detailed focal mechanism descriptions

The detailed focal mechanism descriptions presented in the following pages describe the best (maximum likelihood) focal mechanism together with a couple of important inversion parameters. The moment tensor, the principal axes and the focal planes of the best solution are given. Then we show the epicenter of the event on a map of Hungary and the beach ball representation of the best focal mechanism. The confidence contours of the P and T principal axes are plotted on top of the beach ball illustrating the uncertainty of the retrieved source mechanism.

3.3.1 HEQ-19850815-0428 (Berhida)

EventID:	HEQ-19850815-0428	Inversion method:	jowapo (DC)
Event origin:	1985-08-15 04:28:47	No. of waveforms:	4
m_b:	4.7	No. of polarities:	84
		Date of inversion:	2020-11-28

Centroid: Longitude: 18.110°E Latitude: 47.060°N Depth: 12 km

Moment: $M_0 = 3.647 \times 10^{16}$ Nm $(M_w = 5.01)$

Moment tensor ($\times 10^{16}$ Nm):

$M_{xx} = 3.278$	$M_{xy} = -1.342$	$M_{xz} = 0.439$
	$M_{yy} = -3.190$	$M_{yz} = -0.920$
		$M_{zz} = -0.088$

Principal axes:

Axis	Value ($\times 10^{16}$ Nm)	Azimuth (°)	Plunge* (°)
T	3.647	168	−10
N	0.000	43	−74
P	−3.647	260	−13

*Plunge is positive downwards and negative upwards.

Nodal planes:

Plane	Strike	Dip	Rake
NP1	214°	88°	-164°
NP2	123°	74°	-3°

Percentages:

DC:	100
CLVD:	–
ISO:	–

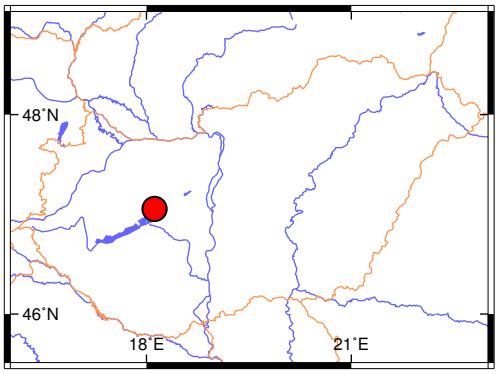

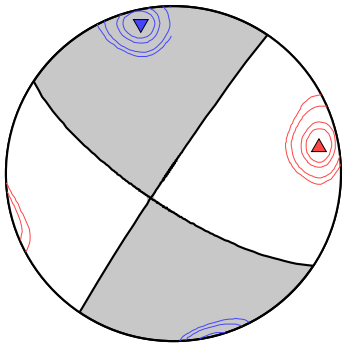

Left: Epicenter location. *Right:* Beach ball representation of the obtained source mechanism. Compressional quadrants of the optimal solution are shaded. Contours represent the 50, 68, 90 and 95% confidence zones for the P (red triangle) and T (blue inverse triangle) principal axes. Equal area projection of lower hemisphere is used.

3.3.2 HEQ-19950609-1557 (Szabadszállás)

EventID:	HEQ-19950609-1557	Inversion method:	mcmt (full MT)
Event origin:	1995-06-09 15:57:02	No. of waveforms:	8
M_L:	1.6	No. of polarities:	–
		Date of inversion:	2018-08-15

Centroid: Longitude: 19.262°E Latitude: 46.924°N Depth: 13 km

Moment: $M_0 = 2.071 \times 10^{12}$ Nm $(M_w = 2.18)$

Moment tensor ($\times 10^{12}$ Nm):

$M_{xx} = 0.579$	$M_{xy} = -1.853$	$M_{xz} = -0.361$
	$M_{yy} = -0.723$	$M_{yz} = 0.150$
		$M_{zz} = -0.014$

Principal axes:

Axis	Value ($\times 10^{12}$ Nm)	Azimuth (°)	Plunge* (°)
T	1.966	325	−11
N	−0.083	312	79
P	−2.040	234	−2

*Plunge is positive downwards and negative upwards.

Nodal planes:

Plane	Strike	Dip	Rake
NP1	280°	84°	10°
NP2	189°	81°	174°

Percentages:

DC:	94
CLVD:	3
ISO:	-3

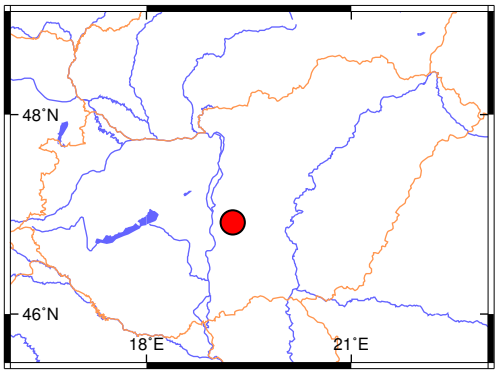

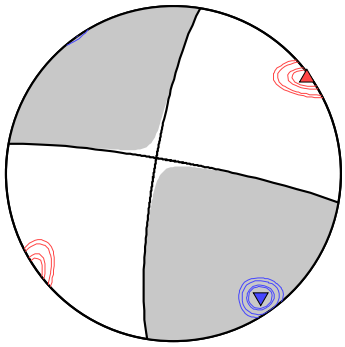

Left: Epicenter location. *Right:* Beach ball representation of the obtained source mechanism. Compressional quadrants of the optimal solution are shaded. Contours represent the 50, 68, 90 and 95% confidence zones for the P (red triangle) and T (blue inverse triangle) principal axes. Equal area projection of lower hemisphere is used.

3.3.3 HEQ-19960328-0631 (Szabadszállás)

EventID:	HEQ-19960328-0631	Inversion method:	mcmt (full MT)
Event origin:	1996-03-28 06:31:22	No. of waveforms:	11
M_L:	3.0	No. of polarities:	–
		Date of inversion:	2018-08-15

Centroid: Longitude: 19.252°E Latitude: 46.909°N Depth: 11 km

Moment: $M_0 = 2.835 \times 10^{13}$ Nm $(M_w = 2.94)$

Moment tensor ($\times 10^{13}$ Nm):

$M_{xx} = 0.180$	$M_{xy} = -2.762$	$M_{xz} = 0.033$
	$M_{yy} = -0.087$	$M_{yz} = 0.408$
		$M_{zz} = 0.024$

Principal axes:

Axis	Value ($\times 10^{13}$ Nm)	Azimuth (°)	Plunge* (°)
T	2.835	316	−5
N	0.036	188	−82
P	−2.755	47	−7

*Plunge is positive downwards and negative upwards.

Nodal planes:

Plane	Strike	Dip	Rake
NP1	1°	89°	-172°
NP2	271°	82°	-1°

Percentages:

DC:	98
CLVD:	1
ISO:	1

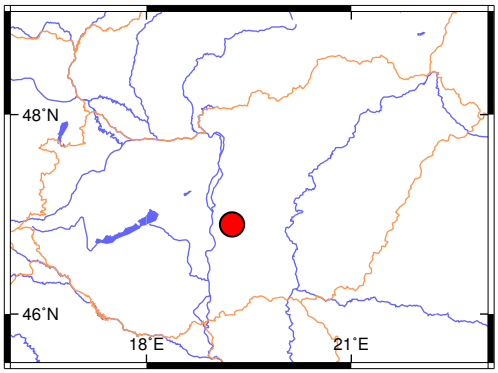

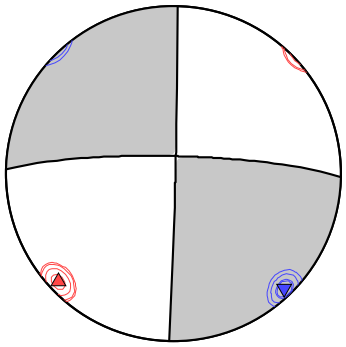

Left: Epicenter location. *Right:* Beach ball representation of the obtained source mechanism. Compressional quadrants of the optimal solution are shaded. Contours represent the 50, 68, 90 and 95% confidence zones for the P (red triangle) and T (blue inverse triangle) principal axes. Equal area projection of lower hemisphere is used.

3.3.4 HEQ-19970523-2340 (Zámoly)

EventID:	HEQ-19970523-2340	Inversion method:	jowapo (DC)
Event origin:	1997-05-23 23:40:18	No. of waveforms:	10
M_L:	1.9	No. of polarities:	4
		Date of inversion:	2019-03-04

Centroid: Longitude: 18.486°E Latitude: 47.358°N Depth: 12 km

Moment: $M_0 = 2.069 \times 10^{12}$ Nm $(M_w = 2.18)$

Moment tensor ($\times 10^{12}$ Nm):

$M_{xx} = 0.555$	$M_{xy} = -0.960$	$M_{xz} = -1.306$
	$M_{yy} = -1.418$	$M_{yz} = -0.350$
		$M_{zz} = 0.863$

Principal axes:

Axis	Value ($\times 10^{12}$ Nm)	Azimuth (°)	Plunge* (°)
T	2.069	350	−46
N	−0.000	316	39
P	−2.069	241	−18

*Plunge is positive downwards and negative upwards.

Nodal planes:

Plane	Strike	Dip	Rake
NP1	302°	73°	49°
NP2	194°	44°	155°

Percentages:

DC:	100
CLVD:	–
ISO:	–

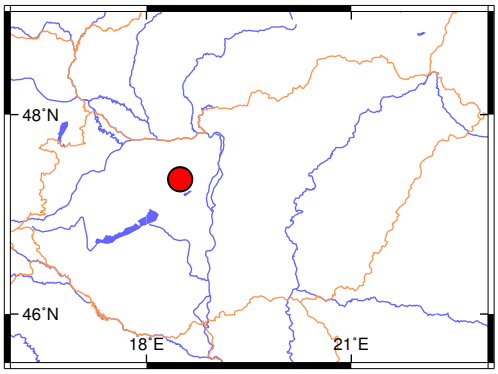

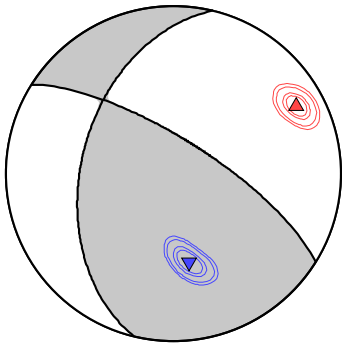

Left: Epicenter location. *Right:* Beach ball representation of the obtained source mechanism. Compressional quadrants of the optimal solution are shaded. Contours represent the 50, 68, 90 and 95% confidence zones for the P (red triangle) and T (blue inverse triangle) principal axes. Equal area projection of lower hemisphere is used.

3.3.5 HEQ-19971127-1040 (Nyáregyháza)

EventID:	HEQ-19971127-1040	Inversion method:	jowapo (DC)
Event origin:	1997-11-27 10:40:56	No. of waveforms:	5
M_L:	2.5	No. of polarities:	6
		Date of inversion:	2020-02-26

Centroid: Longitude: 19.424°E Latitude: 47.252°N Depth: 13 km

Moment: $M_0 = 3.448 \times 10^{13}$ Nm $(M_w = 2.99)$

Moment tensor ($\times 10^{13}$ Nm):

$M_{xx} = -1.755$	$M_{xy} = -1.573$	$M_{xz} = 1.716$
	$M_{yy} = -1.123$	$M_{yz} = 0.395$
		$M_{zz} = 2.878$

Principal axes:

Axis	Value ($\times 10^{13}$ Nm)	Azimuth (°)	Plunge* (°)
T	3.448	175	−71
N	−0.000	123	12
P	−3.448	36	−14

*Plunge is positive downwards and negative upwards.

Nodal planes:

Plane	Strike	Dip	Rake
NP1	116°	60°	76°
NP2	322°	32°	113°

Percentages:

DC:	100
CLVD:	–
ISO:	–

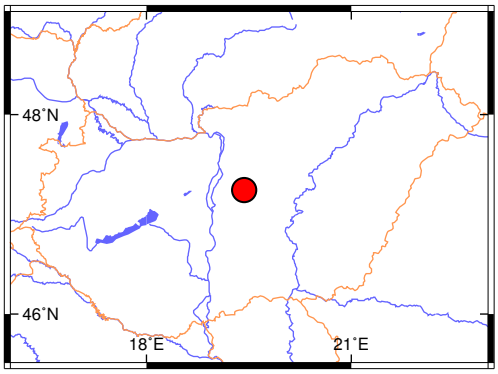

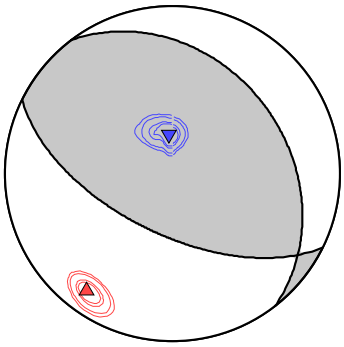

Left: Epicenter location. *Right:* Beach ball representation of the obtained source mechanism. Compressional quadrants of the optimal solution are shaded. Contours represent the 50, 68, 90 and 95% confidence zones for the P (red triangle) and T (blue inverse triangle) principal axes. Equal area projection of lower hemisphere is used.

3.3.6 HEQ-19980508-0406 (Budakeszi)

EventID:	HEQ-19980508-0406	Inversion method:	jowapo (DC)
Event origin:	1998-05-08 04:06:54	No. of waveforms:	6
M_L:	2.0	No. of polarities:	3
		Date of inversion:	2020-02-28

Centroid: Longitude: 18.933°E Latitude: 47.516°N Depth: 9 km

Moment: $M_0 = 5.183 \times 10^{12}$ Nm $(M_w = 2.44)$

Moment tensor ($\times 10^{12}$ Nm):

$M_{xx} = -2.076$	$M_{xy} = -4.194$	$M_{xz} = 0.857$
	$M_{yy} = 2.428$	$M_{yz} = 1.837$
		$M_{zz} = -0.352$

Principal axes:

Axis	Value ($\times 10^{12}$ Nm)	Azimuth (°)	Plunge* (°)
T	5.183	299	−12
N	−0.000	179	−67
P	−5.183	33	−20

*Plunge is positive downwards and negative upwards.

Nodal planes:

Plane	Strike	Dip	Rake
NP1	347°	85°	-157°
NP2	255°	67°	-5°

Percentages:

DC:	100
CLVD:	–
ISO:	–

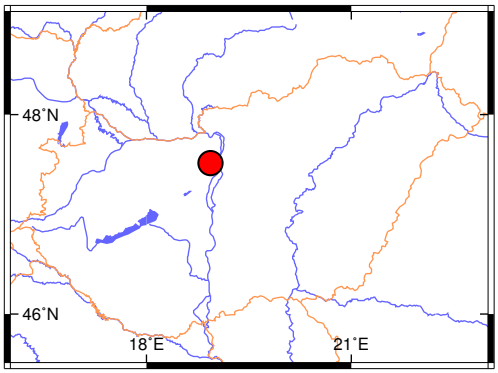

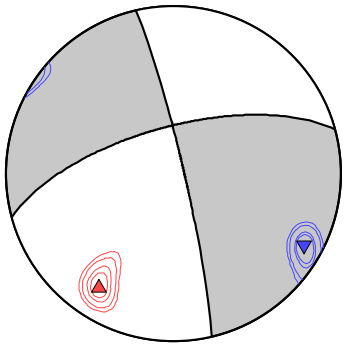

Left: Epicenter location. *Right:* Beach ball representation of the obtained source mechanism. Compressional quadrants of the optimal solution are shaded. Contours represent the 50, 68, 90 and 95% confidence zones for the P (red triangle) and T (blue inverse triangle) principal axes. Equal area projection of lower hemisphere is used.

3.3.7 HEQ-19980628-1219 (Budakeszi)

EventID:	HEQ-19980628-1219	Inversion method:	jowapo (DC)
Event origin:	1998-06-28 12:19:39	No. of waveforms:	7
M_L:	1.4	No. of polarities:	2
		Date of inversion:	2020-02-26

Centroid: Longitude: 18.933°E Latitude: 47.517°N Depth: 8 km

Moment: $M_0 = 7.132 \times 10^{11}$ Nm $(M_w = 1.87)$

Moment tensor ($\times 10^{11}$ Nm):

$M_{xx} = 0.412$	$M_{xy} = -6.096$	$M_{xz} = 3.378$
	$M_{yy} = -1.544$	$M_{yz} = -0.615$
		$M_{zz} = 1.132$

Principal axes:

Axis	Value ($\times 10^{11}$ Nm)	Azimuth (°)	Plunge* (°)
T	7.132	143	−27
N	−0.000	114	60
P	−7.132	47	−13

*Plunge is positive downwards and negative upwards.

Nodal planes:

Plane	Strike	Dip	Rake
NP1	97°	80°	29°
NP2	2°	61°	169°

Percentages:

DC:	100
CLVD:	–
ISO:	–

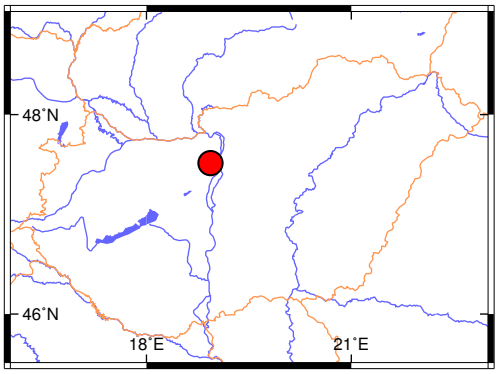

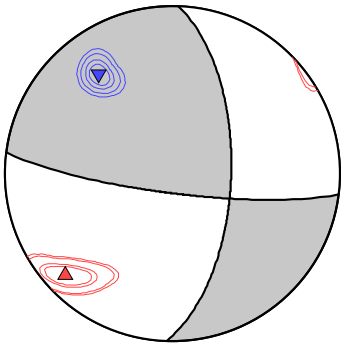

Left: Epicenter location. *Right:* Beach ball representation of the obtained source mechanism. Compressional quadrants of the optimal solution are shaded. Contours represent the 50, 68, 90 and 95% confidence zones for the P (red triangle) and T (blue inverse triangle) principal axes. Equal area projection of lower hemisphere is used.

3.3.8 HEQ-20010525-1515 (Drávaszerdahely)

EventID:	HEQ-20010525-1515	Inversion method:	mcmt (full MT)
Event origin:	2001-05-25 15:15:49	No. of waveforms:	4
M_L:	1.7	No. of polarities:	–
		Date of inversion:	2018-08-15

Centroid: Longitude: 18.107°E Latitude: 45.832°N Depth: 13 km

Moment: $M_0 = 7.736 \times 10^{11}$ Nm $(M_w = 1.89)$

Moment tensor ($\times 10^{11}$ Nm):

$M_{xx} = -0.761$	$M_{xy} = -6.862$	$M_{xz} = 0.412$
	$M_{yy} = 1.230$	$M_{yz} = 1.699$
		$M_{zz} = 0.685$

Principal axes:

Axis	Value ($\times 10^{11}$ Nm)	Azimuth (°)	Plunge* (°)
T	7.327	310	−9
N	0.793	181	−76
P	−6.967	42	−11

*Plunge is positive downwards and negative upwards.

Nodal planes:

Plane	Strike	Dip	Rake
NP1	356°	89°	-166°
NP2	266°	76°	-1°

Percentages:

DC:	84
CLVD:	-11
ISO:	5

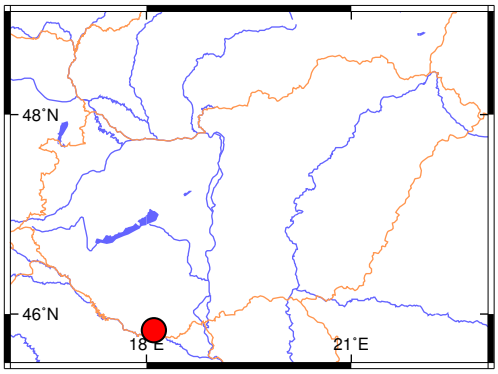

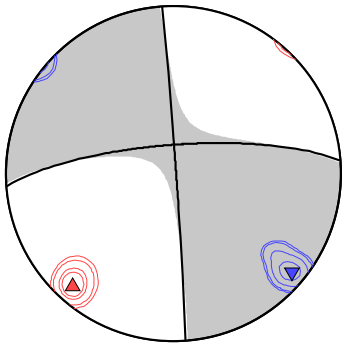

Left: Epicenter location. *Right:* Beach ball representation of the obtained source mechanism. Compressional quadrants of the optimal solution are shaded. Contours represent the 50, 68, 90 and 95% confidence zones for the P (red triangle) and T (blue inverse triangle) principal axes. Equal area projection of lower hemisphere is used.

3.3.9 HEQ-20010608-0958 (Rádfalva)

EventID:	HEQ-20010608-0958	Inversion method:	mcmt (full MT)
Event origin:	2001-06-08 09:58:56	No. of waveforms:	4
M_L:	1.2	No. of polarities:	–
		Date of inversion:	2018-08-15

Centroid: Longitude: 18.114°E Latitude: 45.840°N Depth: 12 km

Moment: $M_0 = 6.410 \times 10^{11}$ Nm $(M_w = 1.84)$

Moment tensor ($\times 10^{11}$ Nm):

$M_{xx} = -0.647$	$M_{xy} = -5.489$	$M_{xz} = 0.295$
	$M_{yy} = 1.156$	$M_{yz} = 1.095$
		$M_{zz} = 0.937$

Principal axes:

Axis	Value ($\times 10^{11}$ Nm)	Azimuth (°)	Plunge* (°)
T	5.902	310	−7
N	0.990	178	−79
P	−5.446	41	−8

*Plunge is positive downwards and negative upwards.

Nodal planes:

Plane	Strike	Dip	Rake
NP1	355°	89°	-169°
NP2	265°	79°	-1°

Percentages:

DC:	77
CLVD:	-16
ISO:	7

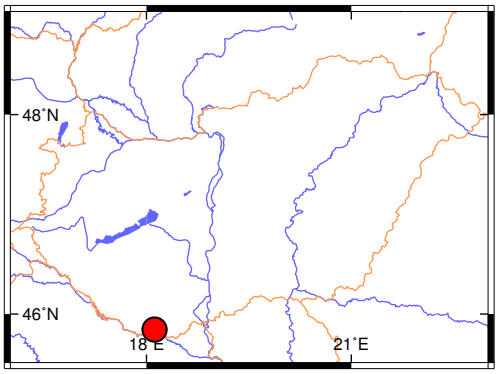

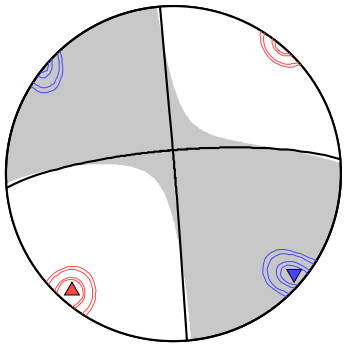

Left: Epicenter location. *Right:* Beach ball representation of the obtained source mechanism. Compressional quadrants of the optimal solution are shaded. Contours represent the 50, 68, 90 and 95% confidence zones for the P (red triangle) and T (blue inverse triangle) principal axes. Equal area projection of lower hemisphere is used.

3.3.10 HEQ-20020222-1152 (Környe)

EventID:	HEQ-20020222-1152	Inversion method:	jowapo (DC)
Event origin:	2002-02-22 11:52:34	No. of waveforms:	6
M_L:	2.9	No. of polarities:	8
		Date of inversion:	2020-03-05

Centroid: Longitude: 18.291°E Latitude: 47.485°N Depth: 6 km

Moment: $M_0 = 1.595 \times 10^{13}$ Nm $(M_w = 2.77)$

Moment tensor ($\times 10^{13}$ Nm):

$M_{xx} = -0.045$	$M_{xy} = -0.521$	$M_{xz} = 0.434$
	$M_{yy} = -1.418$	$M_{yz} = -0.084$
		$M_{zz} = 1.463$

Principal axes:

Axis	Value ($\times 10^{13}$ Nm)	Azimuth (°)	Plunge* (°)
T	1.595	165	−73
N	−0.000	161	17
P	−1.595	71	−1

*Plunge is positive downwards and negative upwards.

Nodal planes:

Plane	Strike	Dip	Rake
NP1	145°	48°	68°
NP2	357°	46°	113°

Percentages:

DC:	100
CLVD:	–
ISO:	–

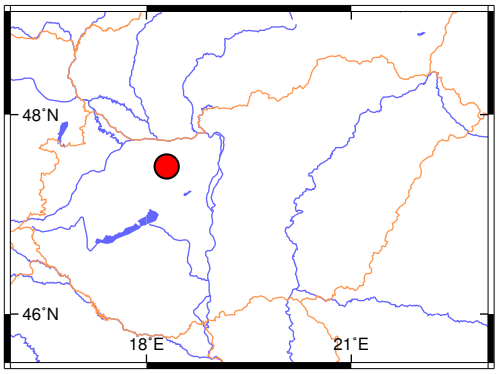

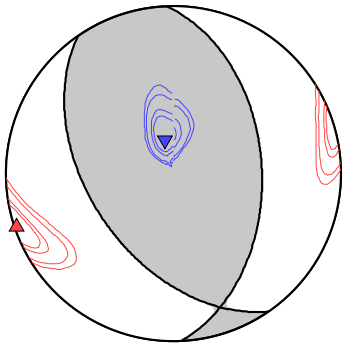

Left: Epicenter location. *Right:* Beach ball representation of the obtained source mechanism. Compressional quadrants of the optimal solution are shaded. Contours represent the 50, 68, 90 and 95% confidence zones for the P (red triangle) and T (blue inverse triangle) principal axes. Equal area projection of lower hemisphere is used.

3.3.11 HEQ-20021012-1849 (Jászapáti)

EventID:	HEQ-20021012-1849	Inversion method:	mcmt (full MT)
Event origin:	2002-10-12 18:49:11	No. of waveforms:	10
M_L:	3.3	No. of polarities:	–
		Date of inversion:	2018-08-15

Centroid: Longitude: 20.062°E Latitude: 47.539°N Depth: 14 km

Moment: $M_0 = 2.607 \times 10^{13}$ Nm $(M_w = 2.91)$

Moment tensor ($\times 10^{13}$ Nm):

$M_{xx} = 0.330$	$M_{xy} = -2.312$	$M_{xz} = 0.011$
	$M_{yy} = 0.195$	$M_{yz} = -0.270$
		$M_{zz} = 0.287$

Principal axes:

Axis	Value ($\times 10^{13}$ Nm)	Azimuth (°)	Plunge* (°)
T	2.593	136	−5
N	0.285	359	−83
P	−2.066	226	−5

*Plunge is positive downwards and negative upwards.

Nodal planes:

Plane	Strike	Dip	Rake
NP1	1°	90°	173°
NP2	91°	83°	0°

Percentages:

DC:	89
CLVD:	-1
ISO:	10

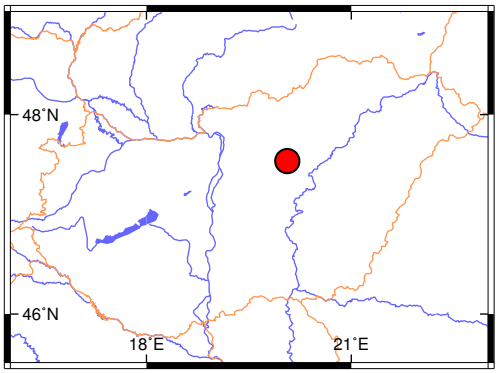

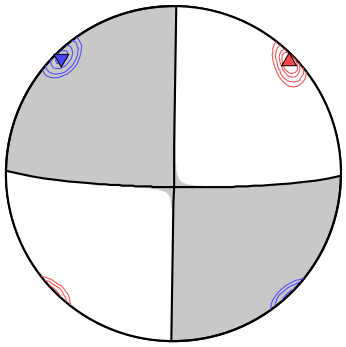

Left: Epicenter location. *Right:* Beach ball representation of the obtained source mechanism. Compressional quadrants of the optimal solution are shaded. Contours represent the 50, 68, 90 and 95% confidence zones for the P (red triangle) and T (blue inverse triangle) principal axes. Equal area projection of lower hemisphere is used.

3.3.12 HEQ-20021023-0252 (Jászapáti)

EventID:	HEQ-20021023-0252	Inversion method:	mcmt (full MT)
Event origin:	2002-10-23 02:52:15	No. of waveforms:	10
M_L:	3.7	No. of polarities:	–
		Date of inversion:	2018-08-15

Centroid: Longitude: 20.041°E Latitude: 47.541°N Depth: 14 km

Moment: $M_0 = 1.475 \times 10^{14}$ Nm $(M_w = 3.41)$

Moment tensor ($\times 10^{14}$ Nm):

$M_{xx} = 0.421$	$M_{xy} = -1.225$	$M_{xz} = -0.106$
	$M_{yy} = 0.053$	$M_{yz} = -0.121$
		$M_{zz} = 0.165$

Principal axes:

Axis	Value ($\times 10^{14}$ Nm)	Azimuth (°)	Plunge* (°)
T	1.475	319	−0
N	0.187	230	82
P	−1.023	229	−8

*Plunge is positive downwards and negative upwards.

Nodal planes:

Plane	Strike	Dip	Rake
NP1	94°	85°	-6°
NP2	185°	85°	-175°

Percentages:

DC:	82
CLVD:	4
ISO:	14

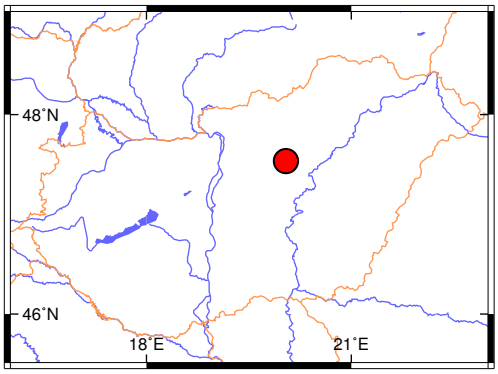

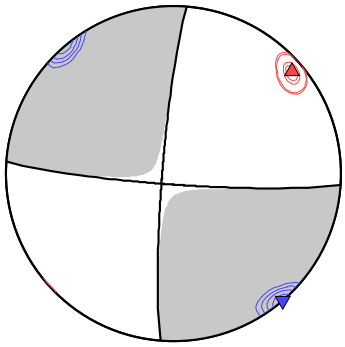

Left: Epicenter location. *Right:* Beach ball representation of the obtained source mechanism. Compressional quadrants of the optimal solution are shaded. Contours represent the 50, 68, 90 and 95% confidence zones for the P (red triangle) and T (blue inverse triangle) principal axes. Equal area projection of lower hemisphere is used.

3.3.13 HEQ-20030621-2005 (Jászapáti)

EventID:	HEQ-20030621-2005	Inversion method:	mcmt (full MT)
Event origin:	2003-06-21 20:05:58	No. of waveforms:	11
M_L:	3.7	No. of polarities:	–
		Date of inversion:	2018-08-15

Centroid: Longitude: 20.058°E Latitude: 47.545°N Depth: 14 km

Moment: $M_0 = 1.059 \times 10^{14}$ Nm $(M_w = 3.32)$

Moment tensor ($\times 10^{14}$ Nm):

$M_{xx} = 0.095$	$M_{xy} = -0.924$	$M_{xz} = 0.054$
	$M_{yy} = 0.162$	$M_{yz} = 0.163$
		$M_{zz} = 0.039$

Principal axes:

Axis	Value ($\times 10^{14}$ Nm)	Azimuth (°)	Plunge* (°)
T	1.059	314	−4
N	0.059	200	−79
P	−0.823	44	−10

*Plunge is positive downwards and negative upwards.

Nodal planes:

Plane	Strike	Dip	Rake
NP1	359°	86°	-170°
NP2	269°	80°	-4°

Percentages:

DC:	83
CLVD:	8
ISO:	9

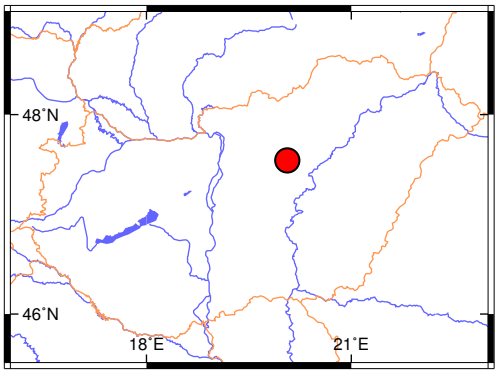

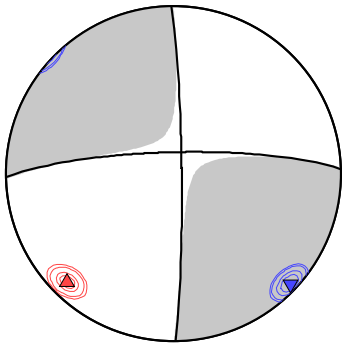

Left: Epicenter location. *Right:* Beach ball representation of the obtained source mechanism. Compressional quadrants of the optimal solution are shaded. Contours represent the 50, 68, 90 and 95% confidence zones for the P (red triangle) and T (blue inverse triangle) principal axes. Equal area projection of lower hemisphere is used.

3.3.14 HEQ-20030627-0119 (Jászapáti)

EventID:	HEQ-20030627-0119	Inversion method:	mcmt (full MT)
Event origin:	2003-06-27 01:19:20	No. of waveforms:	10
M_L:	2.4	No. of polarities:	–
		Date of inversion:	2018-08-15

Centroid: Longitude: 19.998°E Latitude: 47.531°N Depth: 10 km

Moment: $M_0 = 4.275 \times 10^{12}$ Nm $(M_w = 2.39)$

Moment tensor ($\times 10^{12}$ Nm):

$M_{xx} = 0.380$	$M_{xy} = -3.873$	$M_{xz} = -0.059$
	$M_{yy} = -1.050$	$M_{yz} = -0.060$
		$M_{zz} = 0.038$

Principal axes:

Axis	Value ($\times 10^{12}$ Nm)	Azimuth (°)	Plunge* (°)
T	3.603	320	−0
N	0.040	236	89
P	−4.275	230	−1

*Plunge is positive downwards and negative upwards.

Nodal planes:

Plane	Strike	Dip	Rake
NP1	95°	89°	-1°
NP2	185°	89°	-179°

Percentages:

DC:	83
CLVD:	-12
ISO:	-5

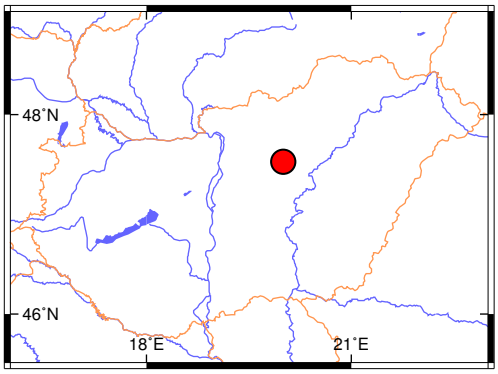

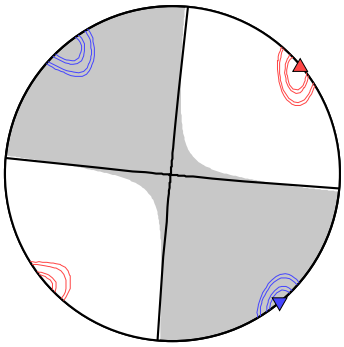

Left: Epicenter location. *Right:* Beach ball representation of the obtained source mechanism. Compressional quadrants of the optimal solution are shaded. Contours represent the 50, 68, 90 and 95% confidence zones for the P (red triangle) and T (blue inverse triangle) principal axes. Equal area projection of lower hemisphere is used.

3.3.15 HEQ-20030831-2257 (Kővágótöttös)

EventID:	HEQ-20030831-2257	Inversion method:	jowapo (DC)
Event origin:	2003-08-31 22:57:21	No. of waveforms:	10
M_L:	1.9	No. of polarities:	5
		Date of inversion:	2019-02-20

Centroid: Longitude: 18.127°E Latitude: 46.105°N Depth: 4 km

Moment: $M_0 = 1.461 \times 10^{13}$ Nm $(M_w = 2.74)$

Moment tensor ($\times 10^{13}$ Nm):

$M_{xx} = 0.657$	$M_{xy} = 0.861$	$M_{xz} = -0.431$
	$M_{yy} = -0.928$	$M_{yz} = -0.723$
		$M_{zz} = 0.271$

Principal axes:

Axis	Value ($\times 10^{13}$ Nm)	Azimuth (°)	Plunge* (°)
T	1.461	30	−32
N	0.000	354	53
P	−1.461	289	−18

*Plunge is positive downwards and negative upwards.

Nodal planes:

Plane	Strike	Dip	Rake
NP1	342°	81°	36°
NP2	245°	54°	169°

Percentages:

DC:	100
CLVD:	–
ISO:	–

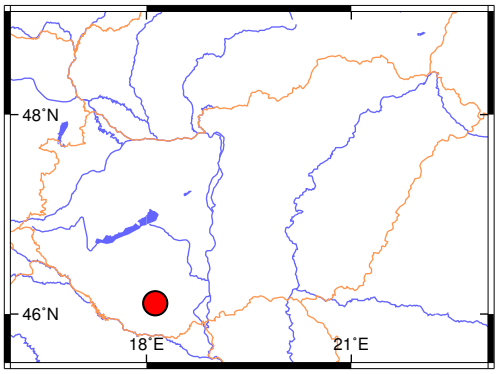

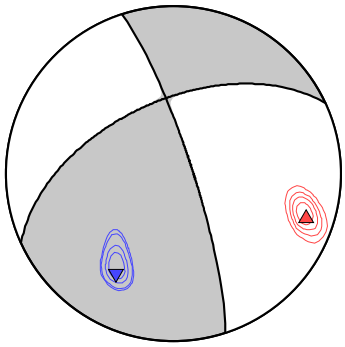

Left: Epicenter location. *Right:* Beach ball representation of the obtained source mechanism. Compressional quadrants of the optimal solution are shaded. Contours represent the 50, 68, 90 and 95% confidence zones for the P (red triangle) and T (blue inverse triangle) principal axes. Equal area projection of lower hemisphere is used.

3.3.16 HEQ-20031231-2043 (Magyarsarlós)

EventID:	HEQ-20031231-2043	Inversion method:	jowapo (DC)
Event origin:	2003-12-31 20:43:49	No. of waveforms:	8
M_L:	2.6	No. of polarities:	7
		Date of inversion:	2020-02-25

Centroid: Longitude: 18.288°E Latitude: 46.037°N Depth: 13 km

Moment: $M_0 = 9.193 \times 10^{12}$ Nm $(M_w = 2.61)$

Moment tensor ($\times 10^{12}$ Nm):

$M_{xx} = -4.161$	$M_{xy} = -7.270$	$M_{xz} = -3.719$
	$M_{yy} = 3.930$	$M_{yz} = 1.192$
		$M_{zz} = 0.231$

Principal axes:

Axis	Value ($\times 10^{12}$ Nm)	Azimuth (°)	Plunge* (°)
T	9.193	303	−19
N	0.000	259	65
P	−9.193	208	−16

*Plunge is positive downwards and negative upwards.

Nodal planes:

Plane	Strike	Dip	Rake
NP1	256°	88°	25°
NP2	165°	65°	178°

Percentages:

DC:	100
CLVD:	–
ISO:	–

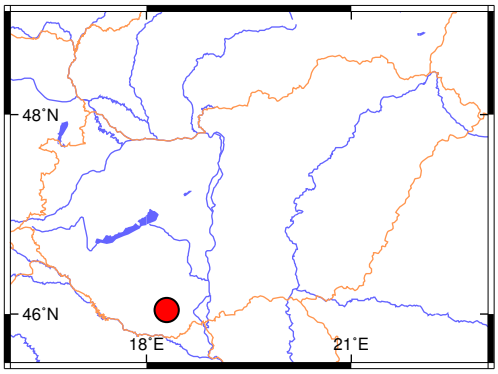

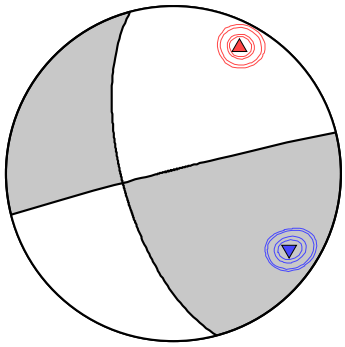

Left: Epicenter location. *Right:* Beach ball representation of the obtained source mechanism. Compressional quadrants of the optimal solution are shaded. Contours represent the 50, 68, 90 and 95% confidence zones for the P (red triangle) and T (blue inverse triangle) principal axes. Equal area projection of lower hemisphere is used.

3.3.17 HEQ-20031231-2136 (Kozármisleny)

EventID:	HEQ-20031231-2136	Inversion method:	jowapo (DC)
Event origin:	2003-12-31 21:36:02	No. of waveforms:	8
M_L:	1.6	No. of polarities:	3
		Date of inversion:	2020-02-25

Centroid: Longitude: 18.283°E Latitude: 46.037°N Depth: 10 km

Moment: $M_0 = 1.197 \times 10^{12}$ Nm $(M_w = 2.02)$

Moment tensor ($\times 10^{12}$ Nm):

$M_{xx} = -0.520$	$M_{xy} = -0.846$	$M_{xz} = -0.668$
	$M_{yy} = 0.299$	$M_{yz} = 0.258$
		$M_{zz} = 0.221$

Principal axes:

Axis	Value ($\times 10^{12}$ Nm)	Azimuth (°)	Plunge* (°)
T	1.197	309	−32
N	0.000	271	51
P	−1.197	207	−19

*Plunge is positive downwards and negative upwards.

Nodal planes:

Plane	Strike	Dip	Rake
NP1	260°	81°	38°
NP2	164°	53°	169°

Percentages:

DC:	100
CLVD:	–
ISO:	–

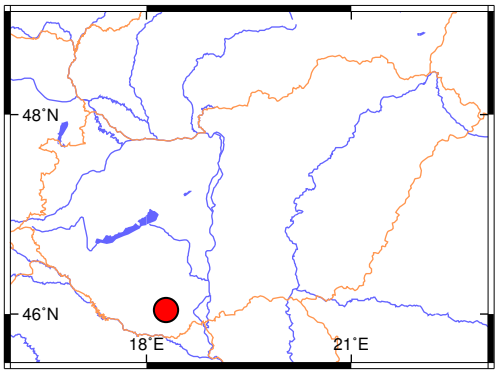

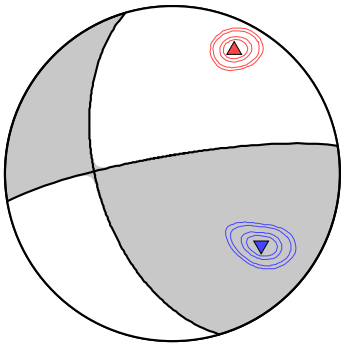

Left: Epicenter location. *Right:* Beach ball representation of the obtained source mechanism. Compressional quadrants of the optimal solution are shaded. Contours represent the 50, 68, 90 and 95% confidence zones for the P (red triangle) and T (blue inverse triangle) principal axes. Equal area projection of lower hemisphere is used.

3.3.18 HEQ-20040619-1048 (Portelek)

EventID:	HEQ-20040619-1048	Inversion method:	jowapo (DC)
Event origin:	2004-06-19 10:48:07	No. of waveforms:	5
M_L:	2.5	No. of polarities:	5
		Date of inversion:	2020-03-08

Centroid: Longitude: 19.930°E Latitude: 47.390°N Depth: 13 km

Moment: $M_0 = 9.415 \times 10^{12}$ Nm $(M_w = 2.62)$

Moment tensor ($\times 10^{12}$ Nm):

$M_{xx} = -1.376$	$M_{xy} = -8.000$	$M_{xz} = 0.050$
	$M_{yy} = 0.948$	$M_{yz} = 4.812$
		$M_{zz} = 0.428$

Principal axes:

Axis	Value ($\times 10^{12}$ Nm)	Azimuth (°)	Plunge* (°)
T	9.415	306	−23
N	−0.000	171	−59
P	−9.415	45	−19

*Plunge is positive downwards and negative upwards.

Nodal planes:

Plane	Strike	Dip	Rake
NP1	175°	87°	149°
NP2	267°	59°	3°

Percentages:

DC:	100
CLVD:	–
ISO:	–

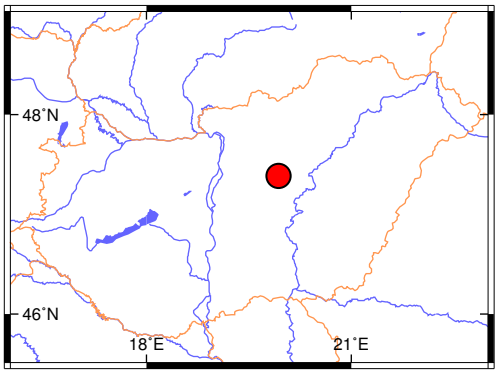

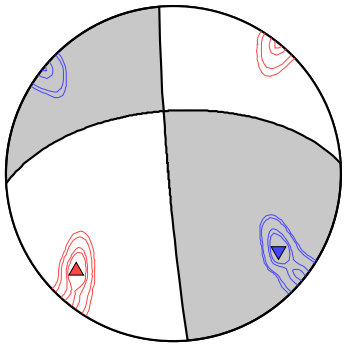

Left: Epicenter location. *Right:* Beach ball representation of the obtained source mechanism. Compressional quadrants of the optimal solution are shaded. Contours represent the 50, 68, 90 and 95% confidence zones for the P (red triangle) and T (blue inverse triangle) principal axes. Equal area projection of lower hemisphere is used.

3.3.19 HEQ-20040929-0046 (Buják)

EventID:	HEQ-20040929-0046	Inversion method:	mcmt (deviatoric MT)
Event origin:	2004-09-29 00:46:27	No. of waveforms:	9
M_L:	2.0	No. of polarities:	–
		Date of inversion:	2020-04-14

Centroid: Longitude: 19.527°E Latitude: 47.897°N Depth: 8 km

Moment: $M_0 = 4.345 \times 10^{12}$ Nm $(M_w = 2.39)$

Moment tensor ($\times 10^{12}$ Nm):

$M_{xx} = -3.623$	$M_{xy} = -1.011$	$M_{xz} = 1.617$
	$M_{yy} = 0.130$	$M_{yz} = 1.326$
		$M_{zz} = 3.493$

Principal axes:

Axis	Value ($\times 10^{12}$ Nm)	Azimuth (°)	Plunge* (°)
T	4.150	239	−72
N	0.196	110	−12
P	−4.345	17	−14

*Plunge is positive downwards and negative upwards.

Nodal planes:

Plane	Strike	Dip	Rake
NP1	117°	60°	104°
NP2	271°	33°	68°

Percentages:

DC:	91
CLVD:	-9
ISO:	–

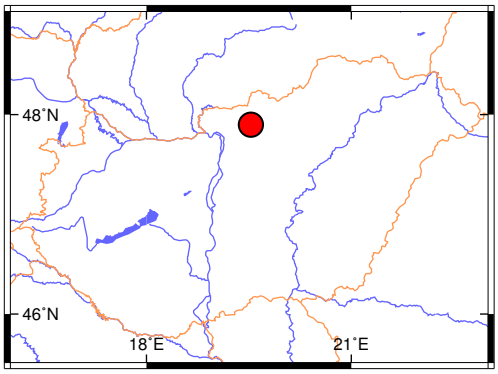

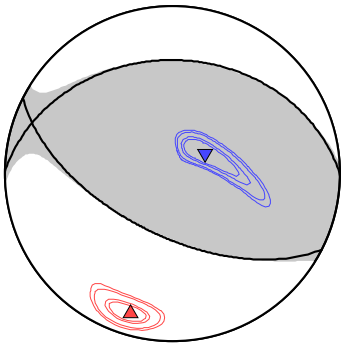

Left: Epicenter location. *Right:* Beach ball representation of the obtained source mechanism. Compressional quadrants of the optimal solution are shaded. Contours represent the 50, 68, 90 and 95% confidence zones for the P (red triangle) and T (blue inverse triangle) principal axes. Equal area projection of lower hemisphere is used.

3.3.20 HEQ-20061123-0715 (Beregsurány)

EventID:	HEQ-20061123-0715	Inversion method:	mcmt (full MT)
Event origin:	2006-11-23 07:15:21	No. of waveforms:	23
M_L:	4.5	No. of polarities:	–
		Date of inversion:	2020-04-24

Centroid: Longitude: 22.541°E Latitude: 48.218°N Depth: 11 km

Moment: $M_0 = 1.498 \times 10^{15}$ Nm $(M_w = 4.08)$

Moment tensor ($\times 10^{15}$ Nm):

$M_{xx} = -0.240$	$M_{xy} = -0.636$	$M_{xz} = 0.417$
	$M_{yy} = -0.600$	$M_{yz} = 0.210$
		$M_{zz} = 1.359$

Principal axes:

Axis	Value ($\times 10^{15}$ Nm)	Azimuth (°)	Plunge* (°)
T	1.463	187	−77
N	0.208	140	9
P	−1.152	51	−10

*Plunge is positive downwards and negative upwards.

Nodal planes:

Plane	Strike	Dip	Rake
NP1	134°	55°	79°
NP2	333°	36°	106°

Percentages:

DC:	84
CLVD:	-5
ISO:	11

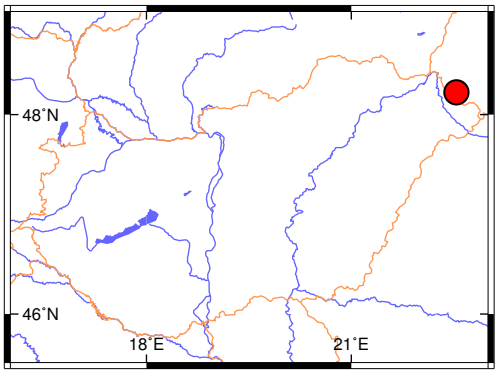

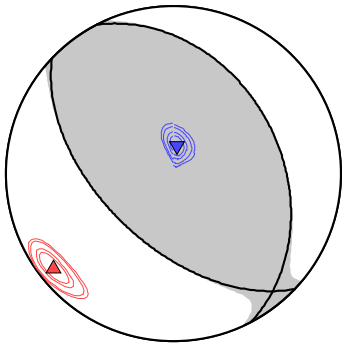

Left: Epicenter location. *Right:* Beach ball representation of the obtained source mechanism. Compressional quadrants of the optimal solution are shaded. Contours represent the 50, 68, 90 and 95% confidence zones for the P (red triangle) and T (blue inverse triangle) principal axes. Equal area projection of lower hemisphere is used.

3.3.21 HEQ-20061231-1339 (Gyömrő)

EventID:	HEQ-20061231-1339	Inversion method:	jowapo (DC)
Event origin:	2006-12-31 13:39:23	No. of waveforms:	14
M_L:	4.1	No. of polarities:	11
		Date of inversion:	2020-04-17

Centroid: Longitude: 19.331°E Latitude: 47.410°N Depth: 6 km

Moment: $M_0 = 1.164 \times 10^{14}$ Nm $(M_w = 3.34)$

Moment tensor ($\times 10^{14}$ Nm):

$M_{xx} = 0.845$	$M_{xy} = -0.792$	$M_{xz} = 0.107$
	$M_{yy} = -0.812$	$M_{yz} = 0.170$
		$M_{zz} = -0.033$

Principal axes:

Axis	Value ($\times 10^{14}$ Nm)	Azimuth (°)	Plunge* (°)
T	1.164	158	−2
N	0.000	78	80
P	−1.164	68	−10

*Plunge is positive downwards and negative upwards.

Nodal planes:

Plane	Strike	Dip	Rake
NP1	293°	84°	-8°
NP2	24°	82°	-174°

Percentages:

DC:	100
CLVD:	–
ISO:	–

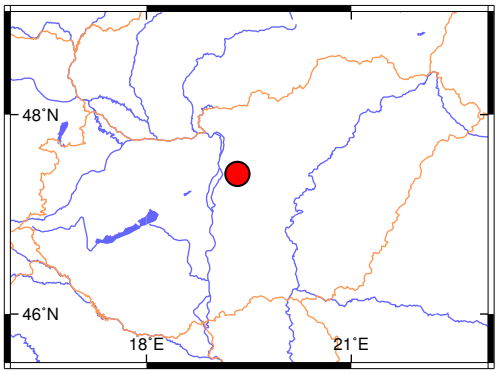

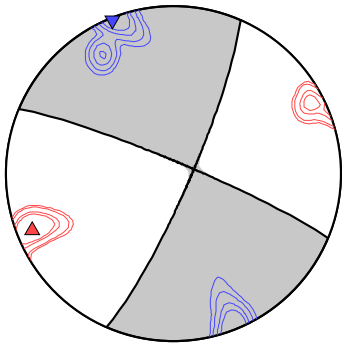

Left: Epicenter location. *Right:* Beach ball representation of the obtained source mechanism. Compressional quadrants of the optimal solution are shaded. Contours represent the 50, 68, 90 and 95% confidence zones for the P (red triangle) and T (blue inverse triangle) principal axes. Equal area projection of lower hemisphere is used.

3.3.22 HEQ-20110129-1741 (Oroszlány)

EventID:	HEQ-20110129-1741	Inversion method:	mcmt (full MT)
Event origin:	2011-01-29 17:41:38	No. of waveforms:	36
M_L:	4.5	No. of polarities:	–
		Date of inversion:	2020-05-24

Centroid: Longitude: 18.375°E Latitude: 47.482°N Depth: 7 km

Moment: $M_0 = 2.048 \times 10^{15}$ Nm $(M_w = 4.17)$

Moment tensor ($\times 10^{15}$ Nm):

$M_{xx} = 0.091$	$M_{xy} = -1.848$	$M_{xz} = 0.184$
	$M_{yy} = 0.083$	$M_{yz} = -0.395$
		$M_{zz} = 0.239$

Principal axes:

Axis	Value ($\times 10^{15}$ Nm)	Azimuth (°)	Plunge* (°)
T	2.029	135	−13
N	0.157	334	−76
P	−1.772	226	−4

*Plunge is positive downwards and negative upwards.

Nodal planes:

Plane	Strike	Dip	Rake
NP1	359°	84°	168°
NP2	91°	78°	6°

Percentages:

DC:	91
CLVD:	-2
ISO:	7

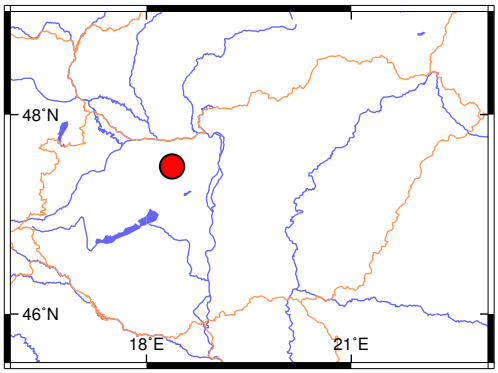

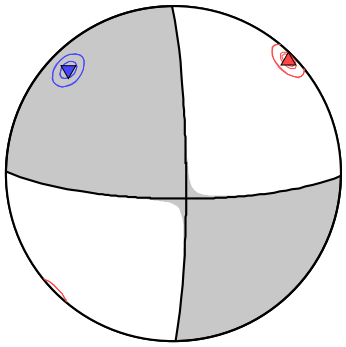

Left: Epicenter location. *Right:* Beach ball representation of the obtained source mechanism. Compressional quadrants of the optimal solution are shaded. Contours represent the 50, 68, 90 and 95% confidence zones for the P (red triangle) and T (blue inverse triangle) principal axes. Equal area projection of lower hemisphere is used.

3.3.23 HEQ-20110130-1334 (Oroszlány)

EventID:	HEQ-20110130-1334	Inversion method:	mcmt (full MT)
Event origin:	2011-01-30 13:34:28	No. of waveforms:	14
M_L:	2.0	No. of polarities:	–
		Date of inversion:	2020-06-05

Centroid: Longitude: 18.366°E Latitude: 47.480°N Depth: 8 km

Moment: $M_0 = 2.031 \times 10^{12}$ Nm $(M_w = 2.17)$

Moment tensor ($\times 10^{12}$ Nm):

$M_{xx} = 1.181$	$M_{xy} = -1.551$	$M_{xz} = 0.093$
	$M_{yy} = -0.890$	$M_{yz} = -0.241$
		$M_{zz} = 0.148$

Principal axes:

Axis	Value ($\times 10^{12}$ Nm)	Azimuth (°)	Plunge* (°)
T	2.031	152	−6
N	0.143	13	−82
P	−1.735	242	−5

*Plunge is positive downwards and negative upwards.

Nodal planes:

Plane	Strike	Dip	Rake
NP1	17°	89°	172°
NP2	107°	82°	1°

Percentages:

DC:	92
CLVD:	1
ISO:	7

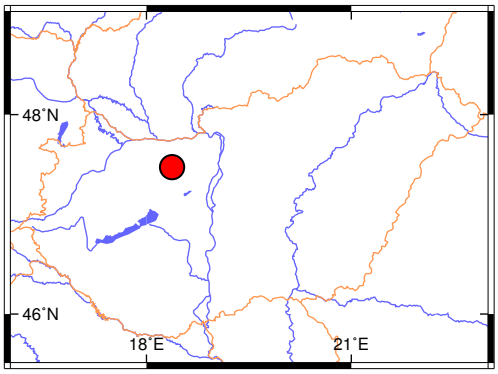

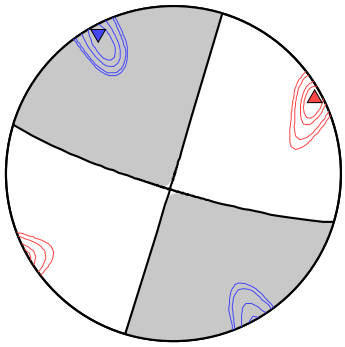

Left: Epicenter location. *Right:* Beach ball representation of the obtained source mechanism. Compressional quadrants of the optimal solution are shaded. Contours represent the 50, 68, 90 and 95% confidence zones for the P (red triangle) and T (blue inverse triangle) principal axes. Equal area projection of lower hemisphere is used.

3.3.24 HEQ-20110130-2058 (Oroszlány)

EventID:	HEQ-20110130-2058	Inversion method:	mcmt (full MT)
Event origin:	2011-01-30 20:58:45	No. of waveforms:	15
M_L:	2.7	No. of polarities:	–
		Date of inversion:	2020-06-10

Centroid: Longitude: 18.363°E Latitude: 47.471°N Depth: 8 km

Moment: $M_0 = 7.744 \times 10^{12}$ Nm $(M_w = 2.56)$

Moment tensor ($\times 10^{12}$ Nm):

$M_{xx} = -1.286$	$M_{xy} = -6.524$	$M_{xz} = 1.967$
	$M_{yy} = 1.630$	$M_{yz} = 2.014$
		$M_{zz} = -1.398$

Principal axes:

Axis	Value ($\times 10^{12}$ Nm)	Azimuth (°)	Plunge* (°)
T	6.873	308	−3
N	−0.181	212	−66
P	−7.744	39	−24

*Plunge is positive downwards and negative upwards.

Nodal planes:

Plane	Strike	Dip	Rake
NP1	356°	75°	-161°
NP2	261°	72°	-16°

Percentages:

DC:	91
CLVD:	-4
ISO:	-5

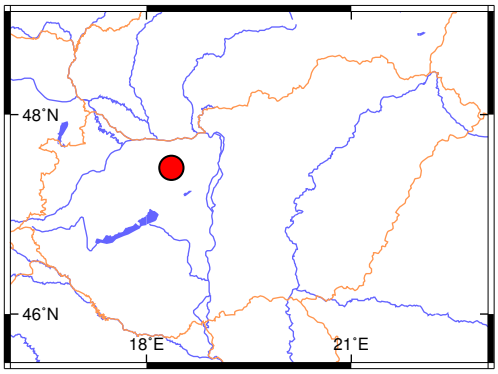

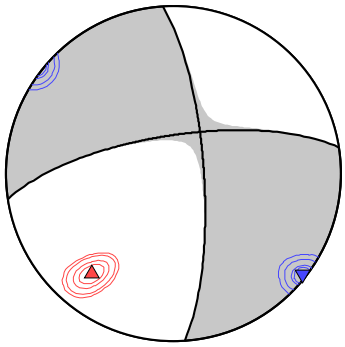

Left: Epicenter location. *Right:* Beach ball representation of the obtained source mechanism. Compressional quadrants of the optimal solution are shaded. Contours represent the 50, 68, 90 and 95% confidence zones for the P (red triangle) and T (blue inverse triangle) principal axes. Equal area projection of lower hemisphere is used.

3.3.25 HEQ-20110131-0025 (Oroszlány)

EventID:	HEQ-20110131-0025	Inversion method:	mcmt (full MT)
Event origin:	2011-01-31 00:25:29	No. of waveforms:	14
M_L:	2.4	No. of polarities:	–
		Date of inversion:	2020-06-24

Centroid: Longitude: 18.365°E Latitude: 47.469°N Depth: 8 km

Moment: $M_0 = 5.513 \times 10^{12}$ Nm $(M_w = 2.46)$

Moment tensor ($\times 10^{12}$ Nm):

$M_{xx} = -3.068$	$M_{xy} = -1.878$	$M_{xz} = -0.029$
	$M_{yy} = 0.137$	$M_{yz} = -1.501$
		$M_{zz} = 5.063$

Principal axes:

Axis	Value ($\times 10^{12}$ Nm)	Azimuth (°)	Plunge* (°)
T	5.513	102	−73
N	0.603	297	−17
P	−3.984	206	−4

*Plunge is positive downwards and negative upwards.

Nodal planes:

Plane	Strike	Dip	Rake
NP1	311°	51°	111°
NP2	99°	43°	65°

Percentages:

DC:	83
CLVD:	4
ISO:	13

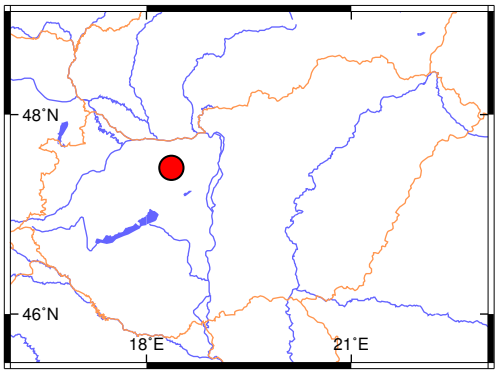

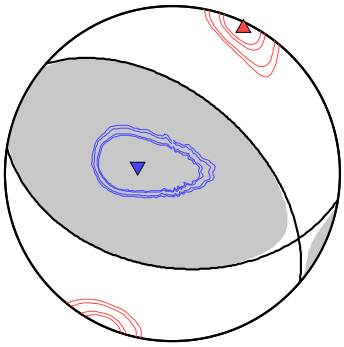

Left: Epicenter location. *Right:* Beach ball representation of the obtained source mechanism. Compressional quadrants of the optimal solution are shaded. Contours represent the 50, 68, 90 and 95% confidence zones for the P (red triangle) and T (blue inverse triangle) principal axes. Equal area projection of lower hemisphere is used.

3.3.26 HEQ-20110311-0145 (Oroszlány)

EventID:	HEQ-20110311-0145	Inversion method:	mcmt (full MT)
Event origin:	2011-03-11 01:45:23	No. of waveforms:	17
M_L:	2.3	No. of polarities:	–
		Date of inversion:	2020-07-01

Centroid: Longitude: 18.365°E Latitude: 47.467°N Depth: 8 km

Moment: $M_0 = 5.372 \times 10^{12}$ Nm $(M_w = 2.45)$

Moment tensor ($\times 10^{12}$ Nm):

$M_{xx} = 2.370$	$M_{xy} = -4.229$	$M_{xz} = 1.484$
	$M_{yy} = -2.237$	$M_{yz} = 1.164$
		$M_{zz} = -0.361$

Principal axes:

Axis	Value ($\times 10^{12}$ Nm)	Azimuth (°)	Plunge* (°)
T	4.975	151	−8
N	0.169	81	69
P	−5.372	58	−19

*Plunge is positive downwards and negative upwards.

Nodal planes:

Plane	Strike	Dip	Rake
NP1	283°	82°	-20°
NP2	16°	71°	-171°

Percentages:

DC:	89
CLVD:	-9
ISO:	-2

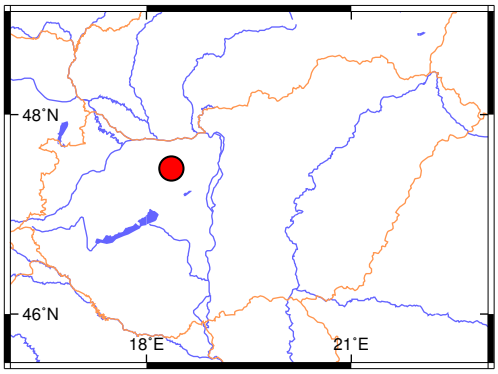

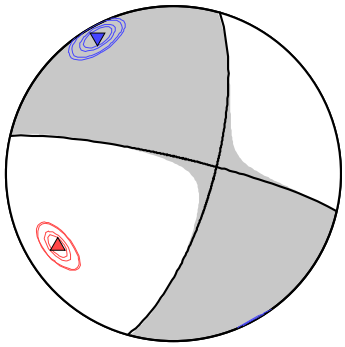

Left: Epicenter location. *Right:* Beach ball representation of the obtained source mechanism. Compressional quadrants of the optimal solution are shaded. Contours represent the 50, 68, 90 and 95% confidence zones for the P (red triangle) and T (blue inverse triangle) principal axes. Equal area projection of lower hemisphere is used.

3.3.27 HEQ-20130422-2228 (Tenk)

EventID:	HEQ-20130422-2228	Inversion method:	mcmt (deviatoric MT)
Event origin:	2013-04-22 22:28:46	No. of waveforms:	32
M_L:	4.8	No. of polarities:	–
		Date of inversion:	2020-07-08

Centroid: Longitude: 20.289°E Latitude: 47.634°N Depth: 3 km

Moment: $M_0 = 5.547 \times 10^{15}$ Nm $(M_w = 4.46)$

Moment tensor ($\times 10^{15}$ Nm):

$M_{xx} = -2.826$	$M_{xy} = -2.829$	$M_{xz} = 0.159$
	$M_{yy} = -2.585$	$M_{yz} = -0.639$
		$M_{zz} = 5.412$

Principal axes:

Axis	Value ($\times 10^{15}$ Nm)	Azimuth (°)	Plunge* (°)
T	5.482	118	−84
N	0.065	314	−6
P	−5.547	224	−2

*Plunge is positive downwards and negative upwards.

Nodal planes:

Plane	Strike	Dip	Rake
NP1	320°	47°	98°
NP2	128°	44°	81°

Percentages:

DC:	98
CLVD:	-2
ISO:	–

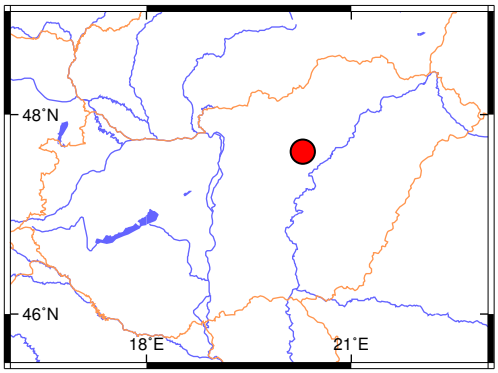

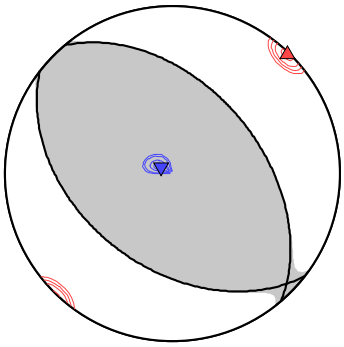

Left: Epicenter location. *Right:* Beach ball representation of the obtained source mechanism. Compressional quadrants of the optimal solution are shaded. Contours represent the 50, 68, 90 and 95% confidence zones for the P (red triangle) and T (blue inverse triangle) principal axes. Equal area projection of lower hemisphere is used.

3.3.28 HEQ-20130605-1845 (Érsekvadkert)

EventID:	HEQ-20130605-1845	Inversion method:	mcmt (full MT)
Event origin:	2013-06-05 18:45:46	No. of waveforms:	36
M_L:	4.1	No. of polarities:	–
		Date of inversion:	2020-07-13

Centroid: Longitude: 19.251°E Latitude: 47.992°N Depth: 3 km

Moment: $M_0 = 7.956 \times 10^{14}$ Nm $(M_w = 3.90)$

Moment tensor ($\times 10^{14}$ Nm):

$M_{xx} = -1.211$	$M_{xy} = -6.492$	$M_{xz} = -0.204$
	$M_{yy} = 3.254$	$M_{yz} = -0.995$
		$M_{zz} = 0.962$

Principal axes:

Axis	Value ($\times 10^{14}$ Nm)	Azimuth (°)	Plunge* (°)
T	7.956	125	−6
N	0.974	353	−82
P	−5.925	216	−6

*Plunge is positive downwards and negative upwards.

Nodal planes:

Plane	Strike	Dip	Rake
NP1	171°	90°	-172°
NP2	80°	82°	-0°

Percentages:

DC:	87
CLVD:	1
ISO:	12

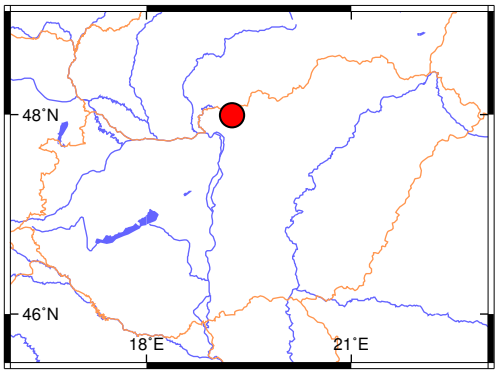

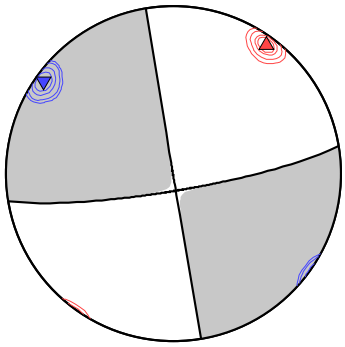

Left: Epicenter location. *Right:* Beach ball representation of the obtained source mechanism. Compressional quadrants of the optimal solution are shaded. Contours represent the 50, 68, 90 and 95% confidence zones for the P (red triangle) and T (blue inverse triangle) principal axes. Equal area projection of lower hemisphere is used.

3.3.29 HEQ-20130702-1907 (Érsekvadkert)

EventID:	HEQ-20130702-1907	Inversion method:	mcmt (full MT)
Event origin:	2013-07-02 19:07:32	No. of waveforms:	26
M_L:	3.4	No. of polarities:	–
		Date of inversion:	2020-07-18

Centroid: Longitude: 19.250°E Latitude: 47.987°N Depth: 3 km

Moment: $M_0 = 3.605 \times 10^{14}$ Nm $(M_w = 3.67)$

Moment tensor ($\times 10^{14}$ Nm):

$M_{xx} = -0.677$	$M_{xy} = -3.092$	$M_{xz} = 0.204$
	$M_{yy} = 1.355$	$M_{yz} = 0.390$
		$M_{zz} = 0.020$

Principal axes:

Axis	Value ($\times 10^{14}$ Nm)	Azimuth (°)	Plunge* (°)
T	3.605	306	−3
N	0.061	193	−82
P	−2.968	36	−8

*Plunge is positive downwards and negative upwards.

Nodal planes:

Plane	Strike	Dip	Rake
NP1	351°	87°	-172°
NP2	261°	82°	-3°

Percentages:

DC:	84
CLVD:	10
ISO:	6

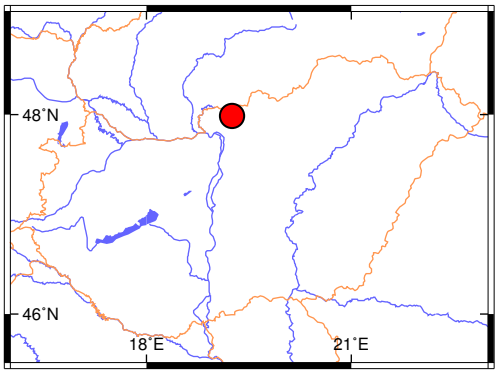

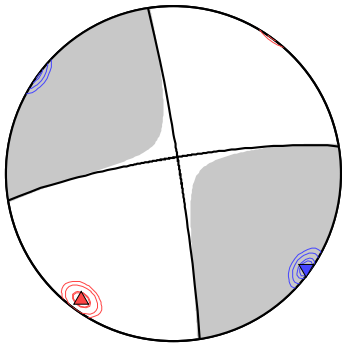

Left: Epicenter location. *Right:* Beach ball representation of the obtained source mechanism. Compressional quadrants of the optimal solution are shaded. Contours represent the 50, 68, 90 and 95% confidence zones for the P (red triangle) and T (blue inverse triangle) principal axes. Equal area projection of lower hemisphere is used.

3.3.30 HEQ-20140119-0134 (Iliny)

EventID:	HEQ-20140119-0134	Inversion method:	mcmt (full MT)
Event origin:	2014-01-19 01:34:34	No. of waveforms:	41
M_L:	4.2	No. of polarities:	–
		Date of inversion:	2020-07-21

Centroid: Longitude: 19.429°E Latitude: 48.035°N Depth: 4 km

Moment: $M_0 = 1.216 \times 10^{15}$ Nm $(M_w = 4.02)$

Moment tensor ($\times 10^{15}$ Nm):

$M_{xx} = -0.373$	$M_{xy} = -0.983$	$M_{xz} = -0.093$
	$M_{yy} = 0.508$	$M_{yz} = -0.331$
		$M_{zz} = 0.087$

Principal axes:

Axis	Value ($\times 10^{15}$ Nm)	Azimuth (°)	Plunge* (°)
T	1.193	122	−12
N	0.097	350	−72
P	−1.068	214	−13

*Plunge is positive downwards and negative upwards.

Nodal planes:

Plane	Strike	Dip	Rake
NP1	168°	89°	-162°
NP2	78°	72°	-1°

Percentages:

DC:	90
CLVD:	-4
ISO:	6

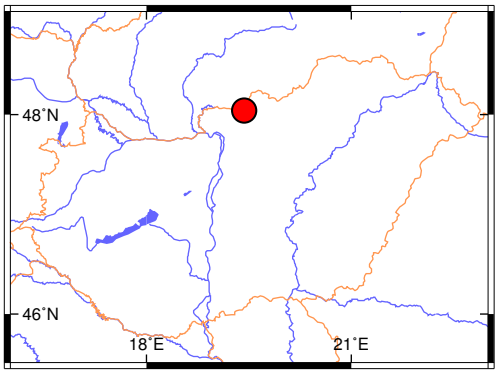

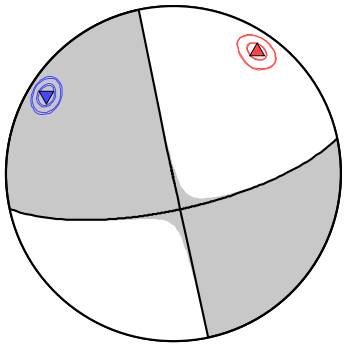

Left: Epicenter location. *Right:* Beach ball representation of the obtained source mechanism. Compressional quadrants of the optimal solution are shaded. Contours represent the 50, 68, 90 and 95% confidence zones for the P (red triangle) and T (blue inverse triangle) principal axes. Equal area projection of lower hemisphere is used.

3.3.31 HEQ-20140119-0148 (Iliny)

EventID:	HEQ-20140119-0148	Inversion method:	jowapo (DC)
Event origin:	2014-01-19 01:48:43	No. of waveforms:	8
M_L:	3.2	No. of polarities:	12
		Date of inversion:	2020-07-23

Centroid: Longitude: 19.424°E Latitude: 48.033°N Depth: 3 km

Moment: $M_0 = 6.266 \times 10^{13}$ Nm $(M_w = 3.16)$

Moment tensor ($\times 10^{13}$ Nm):

$M_{xx} = -2.796$	$M_{xy} = -5.549$	$M_{xz} = 0.675$
	$M_{yy} = 2.619$	$M_{yz} = -0.814$
		$M_{zz} = 0.177$

Principal axes:

Axis	Value ($\times 10^{13}$ Nm)	Azimuth (°)	Plunge* (°)
T	6.266	122	−10
N	−0.000	115	80
P	−6.266	32	−1

*Plunge is positive downwards and negative upwards.

Nodal planes:

Plane	Strike	Dip	Rake
NP1	77°	84°	8°
NP2	347°	82°	174°

Percentages:

DC:	100
CLVD:	–
ISO:	–

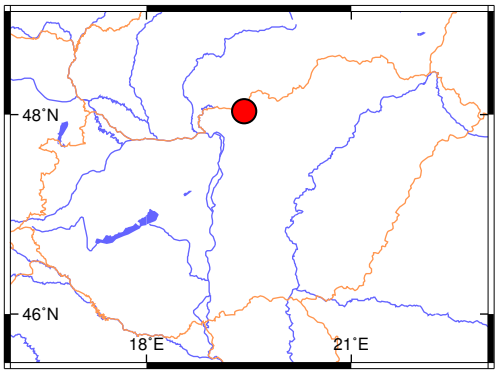

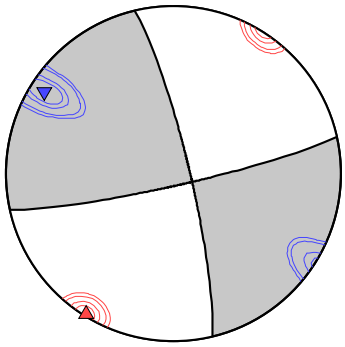

Left: Epicenter location. *Right:* Beach ball representation of the obtained source mechanism. Compressional quadrants of the optimal solution are shaded. Contours represent the 50, 68, 90 and 95% confidence zones for the P (red triangle) and T (blue inverse triangle) principal axes. Equal area projection of lower hemisphere is used.

3.3.32 HEQ-20140803-0148 (Iliny)

EventID:	HEQ-20140803-0148	Inversion method:	jowapo (DC)
Event origin:	2014-08-03 01:48:48	No. of waveforms:	7
M_L:	3.0	No. of polarities:	9
		Date of inversion:	2020-10-14

Centroid: Longitude: 19.423°E Latitude: 48.029°N Depth: 4 km

Moment: $M_0 = 3.686 \times 10^{13}$ Nm $(M_w = 3.01)$

Moment tensor ($\times 10^{13}$ Nm):

$M_{xx} = -2.329$	$M_{xy} = -2.172$	$M_{xz} = 0.679$
	$M_{yy} = -0.164$	$M_{yz} = -1.605$
		$M_{zz} = 2.493$

Principal axes:

Axis	Value ($\times 10^{13}$ Nm)	Azimuth (°)	Plunge* (°)
T	3.686	119	−55
N	−0.000	305	−34
P	−3.686	213	−3

*Plunge is positive downwards and negative upwards.

Nodal planes:

Plane	Strike	Dip	Rake
NP1	331°	57°	132°
NP2	92°	52°	44°

Percentages:

DC:	100
CLVD:	–
ISO:	–

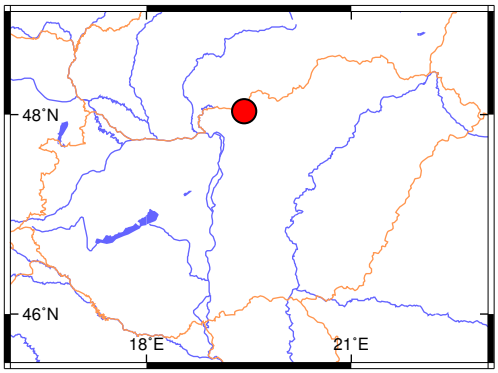

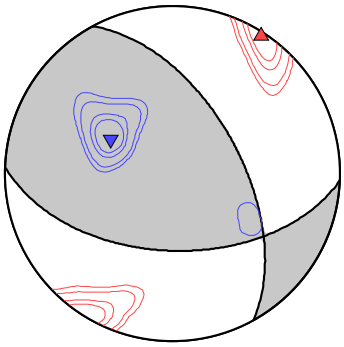

Left: Epicenter location. *Right:* Beach ball representation of the obtained source mechanism. Compressional quadrants of the optimal solution are shaded. Contours represent the 50, 68, 90 and 95% confidence zones for the P (red triangle) and T (blue inverse triangle) principal axes. Equal area projection of lower hemisphere is used.

3.3.33 HEQ-20150101-0643 (Iliny)

EventID:	HEQ-20150101-0643	Inversion method:	jowapo (DC)
Event origin:	2015-01-01 06:43:23	No. of waveforms:	8
M_L:	3.9	No. of polarities:	12
		Date of inversion:	2020-07-27

Centroid: Longitude: 19.431°E Latitude: 48.033°N Depth: 4 km

Moment: $M_0 = 3.964 \times 10^{14}$ Nm $(M_w = 3.70)$

Moment tensor ($\times 10^{14}$ Nm):

$M_{xx} = -1.603$	$M_{xy} = -2.922$	$M_{xz} = -1.957$
	$M_{yy} = 0.176$	$M_{yz} = 1.015$
		$M_{zz} = 1.426$

Principal axes:

Axis	Value ($\times 10^{14}$ Nm)	Azimuth (°)	Plunge* (°)
T	3.964	312	−39
N	0.000	290	49
P	−3.964	213	−11

*Plunge is positive downwards and negative upwards.

Nodal planes:

Plane	Strike	Dip	Rake
NP1	268°	72°	38°
NP2	165°	54°	158°

Percentages:

DC:	100
CLVD:	–
ISO:	–

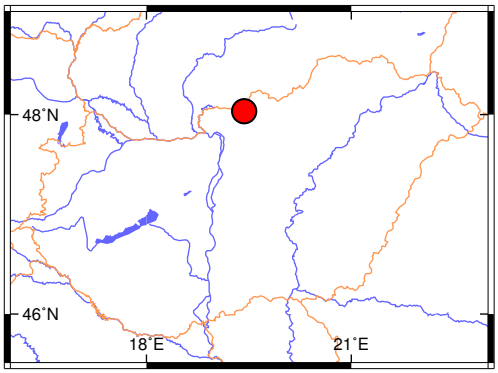

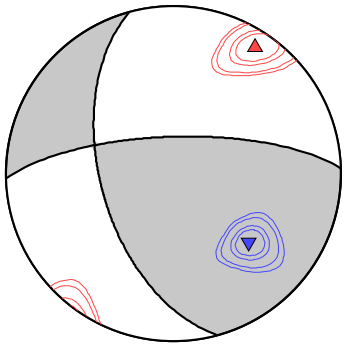

Left: Epicenter location. *Right:* Beach ball representation of the obtained source mechanism. Compressional quadrants of the optimal solution are shaded. Contours represent the 50, 68, 90 and 95% confidence zones for the P (red triangle) and T (blue inverse triangle) principal axes. Equal area projection of lower hemisphere is used.

3.3.34 HEQ-20150101-1045 (Iliny)

EventID:	HEQ-20150101-1045	Inversion method:	jowapo (DC)
Event origin:	2015-01-01 10:45:57	No. of waveforms:	7
M_L:	3.9	No. of polarities:	15
		Date of inversion:	2020-07-29

Centroid: Longitude: 19.422°E Latitude: 48.026°N Depth: 6 km

Moment: $M_0 = 4.718 \times 10^{14}$ Nm $(M_w = 3.75)$

Moment tensor ($\times 10^{14}$ Nm):

$M_{xx} = -1.857$	$M_{xy} = -4.307$	$M_{xz} = 0.008$
	$M_{yy} = 1.833$	$M_{yz} = 0.552$
		$M_{zz} = 0.024$

Principal axes:

Axis	Value ($\times 10^{14}$ Nm)	Azimuth (°)	Plunge* (°)
T	4.718	303	−6
N	0.000	158	−83
P	−4.718	34	−4

*Plunge is positive downwards and negative upwards.

Nodal planes:

Plane	Strike	Dip	Rake
NP1	168°	89°	173°
NP2	258°	83°	1°

Percentages:

DC:	100
CLVD:	–
ISO:	–

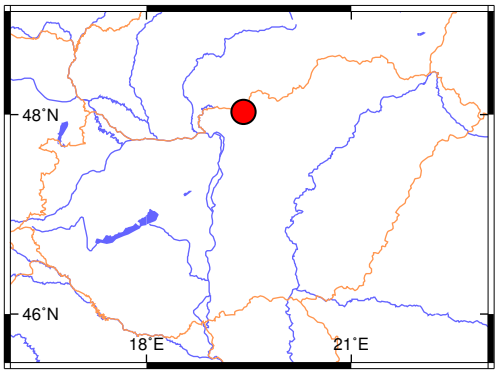

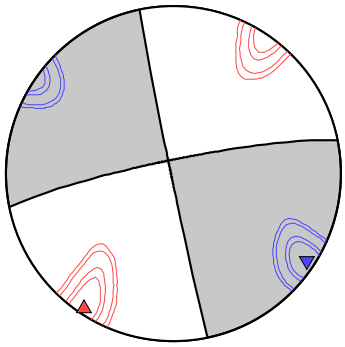

Left: Epicenter location. *Right:* Beach ball representation of the obtained source mechanism. Compressional quadrants of the optimal solution are shaded. Contours represent the 50, 68, 90 and 95% confidence zones for the P (red triangle) and T (blue inverse triangle) principal axes. Equal area projection of lower hemisphere is used.

3.3.35 HEQ-20190217-1440 (Somogyszob)

EventID:	HEQ-20190217-1440	Inversion method:	mcmt (deviatoric MT)
Event origin:	2019-02-17 14:40:45	No. of waveforms:	8
M_L:	2.6	No. of polarities:	–
		Date of inversion:	2019-12-09

Centroid: Longitude: 17.303°E Latitude: 46.312°N Depth: 11 km

Moment: $M_0 = 8.260 \times 10^{12}$ Nm $(M_w = 2.58)$

Moment tensor ($\times 10^{12}$ Nm):

$M_{xx} = -4.650$	$M_{xy} = -3.368$	$M_{xz} = -4.277$
	$M_{yy} = -1.354$	$M_{yz} = -1.893$
		$M_{zz} = 6.004$

Principal axes:

Axis	Value ($\times 10^{12}$ Nm)	Azimuth (°)	Plunge* (°)
T	7.565	15	−71
N	0.695	299	5
P	−8.260	211	−18

*Plunge is positive downwards and negative upwards.

Nodal planes:

Plane	Strike	Dip	Rake
NP1	297°	63°	85°
NP2	128°	27°	100°

Percentages:

DC:	83
CLVD:	-17
ISO:	–

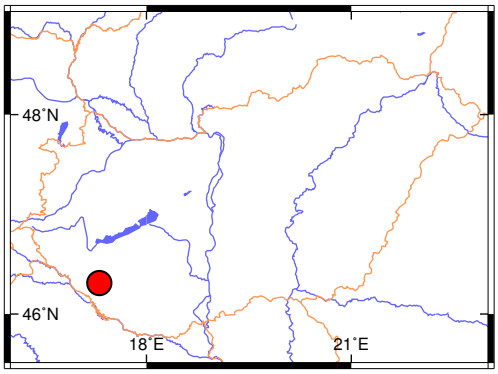

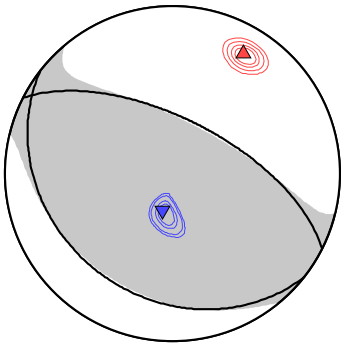

Left: Epicenter location. *Right:* Beach ball representation of the obtained source mechanism. Compressional quadrants of the optimal solution are shaded. Contours represent the 50, 68, 90 and 95% confidence zones for the P (red triangle) and T (blue inverse triangle) principal axes. Equal area projection of lower hemisphere is used.

3.3.36 HEQ-20190307-1907 (Somogyszob)

EventID:	HEQ-20190307-1907	Inversion method:	mcmt (full MT)
Event origin:	2019-03-07 19:07:53	No. of waveforms:	14
M_L:	4.0	No. of polarities:	–
		Date of inversion:	2019-12-09

Centroid: Longitude: 17.302°E Latitude: 46.312°N Depth: 11 km

Moment: $M_0 = 5.443 \times 10^{14}$ Nm $(M_w = 3.79)$

Moment tensor ($\times 10^{14}$ Nm):

$M_{xx} = -3.270$	$M_{xy} = -1.880$	$M_{xz} = -2.158$
	$M_{yy} = -0.945$	$M_{yz} = -2.577$
		$M_{zz} = 3.578$

Principal axes:

Axis	Value ($\times 10^{14}$ Nm)	Azimuth (°)	Plunge* (°)
T	4.940	65	−67
N	−0.134	308	−11
P	−5.443	214	−20

*Plunge is positive downwards and negative upwards.

Nodal planes:

Plane	Strike	Dip	Rake
NP1	313°	66°	102°
NP2	105°	27°	65°

Percentages:

DC:	93
CLVD:	-3
ISO:	-4

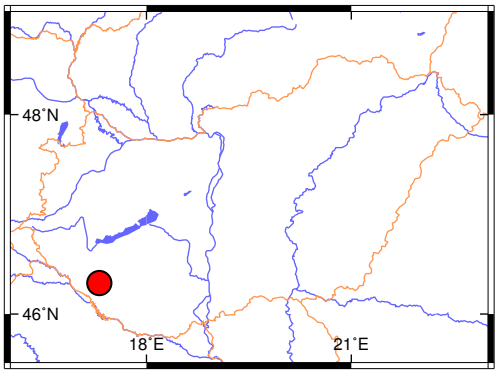

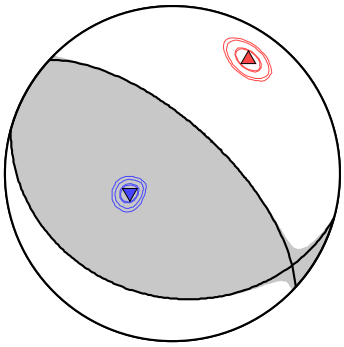

Left: Epicenter location. *Right:* Beach ball representation of the obtained source mechanism. Compressional quadrants of the optimal solution are shaded. Contours represent the 50, 68, 90 and 95% confidence zones for the P (red triangle) and T (blue inverse triangle) principal axes. Equal area projection of lower hemisphere is used.

3.3.37 HEQ-20190405-1352 (Somogyszob)

EventID:	HEQ-20190405-1352	Inversion method:	jowapo (DC)
Event origin:	2019-04-05 13:52:32	No. of waveforms:	6
M_L:	2.3	No. of polarities:	9
		Date of inversion:	2019-11-01

Centroid: Longitude: 17.299°E Latitude: 46.312°N Depth: 11 km

Moment: $M_0 = 1.197 \times 10^{13}$ Nm $(M_w = 2.69)$

Moment tensor ($\times 10^{13}$ Nm):

$M_{xx} = -1.166$	$M_{xy} = -0.067$	$M_{xz} = 0.265$
	$M_{yy} = 0.072$	$M_{yz} = -0.280$
		$M_{zz} = 1.094$

Principal axes:

Axis	Value ($\times 10^{13}$ Nm)	Azimuth (°)	Plunge* (°)
T	1.197	115	−74
N	−0.000	90	14
P	−1.197	2	−6

*Plunge is positive downwards and negative upwards.

Nodal planes:

Plane	Strike	Dip	Rake
NP1	79°	53°	72°
NP2	287°	41°	112°

Percentages:

DC:	100
CLVD:	–
ISO:	–

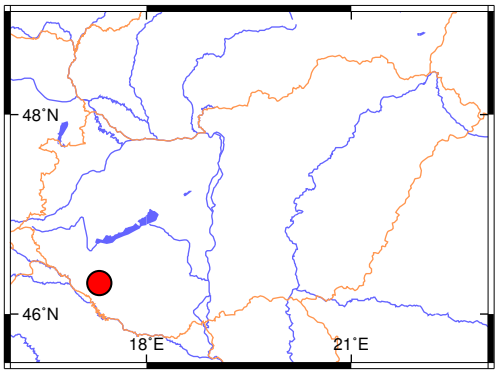

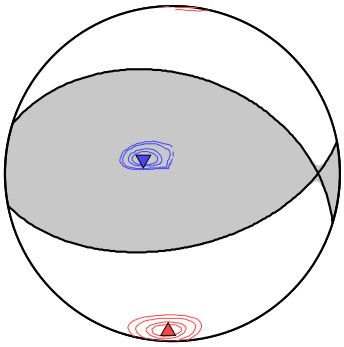

Left: Epicenter location. *Right:* Beach ball representation of the obtained source mechanism. Compressional quadrants of the optimal solution are shaded. Contours represent the 50, 68, 90 and 95% confidence zones for the P (red triangle) and T (blue inverse triangle) principal axes. Equal area projection of lower hemisphere is used.

References

Bada G, Horváth F, Dövényi P, Szafián P, Windhoffer G, Cloetingh S, 2007. Present-day stress field and tectonic inversion in the Pannonian basin. Global and Planetary Change 58, 165-180.

Bowers D, Hudson JA, 1999. Defining the scalar moment of a seismic source with a general moment tensor. Bull. Seismol. Soc. Am. 89, 1390-1394.

Gráczer Z, Wéber Z, 2012. One-dimensional P-wave velocity model for the territory of Hungary from local earthquake data. Acta Geod. Geoph. Hung. 47, 344-357. doi: 10.1556/AGeod.47.2012.3.5

Hanks TC, Kanamori H, 1979. A moment-magnitude scale. J. Geophys. Res. 84, 2348-2350.

Herrmann RB, 2013. Computer programs in seismology: An evolving tool for instruction and research. Seism. Res. Lett. 84, 1081-1088. doi: 10.1785/0220110096

Horváth F, Bada G, Windhoffer G, Csontos L, Dombrádi E, Dövényi P, Fodor L, Grenerczy Gy, Síkhegyi F, Szafián P, Székely B, Timár G, Tóth L, Tóth T, 2006. Atlas of the present-day geodynamics of the Pannonian Basin: Euroconform maps with explanatory text (*in Hungarian with English abstract*). Magyar Geofizika 47, 133-137.

Jost ML, Herrmann RB, 1989. A student's guide to and review of moment tensors. Seism. Res. Lett. 60, 37-57.

Rubinstein RY, Kroese DP, 2008. Simulation and the Monte Carlo Method. John Wiley & Sons, Hoboken, New Jersey.

Sipkin SA, 1993. Display and assessment of earthquake focal mechanisms by vector representation. Bull. Seismol. Soc. Am. 83, 1871-1880.

Vavryčuk V, 2015. Moment tensor decompositions revisited. J. Seismol. 19, 231-252.

Wéber Z, 2005. Probabilistic waveform inversion for focal parameters of local earthquakes. Acta Geod. Geoph. Hung. 40, 229-239.

Wéber Z, 2006. Probabilistic local waveform inversion for moment tensor and hypocentral location. Geophys. J. Int. 165, 607-621. doi: 10.1111/j.1365-246X.2006.02934.x

Wéber Z, 2009. Estimating source time function and moment tensor from moment tensor rate functions by constrained L1 norm minimization. Geophys. J. Int. 178, 889-900. doi: 10.1111/j.1365-246X.2009.04202.x

Wéber Z, 2016a. Probabilistic waveform inversion for 22 earthquake moment tensors in Hungary: new constraints on the tectonic stress pattern inside the Pannonian basin. Geophys. J. Int. 204, 236-249. doi: 10.1093/gji/ggv446

Wéber Z, 2016b. Source parameters for the 2013–2015 earthquake sequence in Nógrád county, Hungary. J. Seismol. 20, 987-999. doi: 10.1007/s10950-016-9576-6

Wéber Z, 2018. Probabilistic joint inversion of waveforms and polarity data for double-couple focal mechanisms of local earthquakes. *Geophys. J. Int.* 213, 1586-1598. doi: 10.1093/gji/ggy096

Wéber Z, Czecze B, Süle B, Bondár I, AlpArray Working Group, 2020. Source analysis of the March 7, 2019 $M_L = 4.0$ Somogyszob, Hungary earthquake sequence. *Acta Geod. Geophys.* 55, 371-387. doi: 10.1007/s40328-020-00311-7

Wéber Z, Süle B, 2014. Source properties of the 29 January 2011 ML 4.5 Oroszlány (Hungary) mainshock and its aftershocks. Bull. Seismol. Soc. Am. 104, 113-127. doi: 10.1785/0120130152